

ABSTRACT

Title of thesis: The Potential Role of Milk-Fat-Globule
Membrane (MFGM) Proteins in Regulating
the Size of Milk-Lipid Droplets

Hyunsu Shin, Master of Science, 2012

Thesis directed By: Professor, Ian. H. Mather,
Department of Animal and Avian Sciences

The aim of this thesis was to identify protein factors that may regulate the size of lipid droplets in milk. To address this hypothesis, the relative amounts of specific MFGM proteins on lipid droplets fractionated according to size were measured. Protein amounts were estimated by quantitative western blotting and confocal microscopy. By quantitative confocal microscopy, small lipid droplets (<1.26 μm) contained more XOR, BTN, adipophilin (ADPH) and fatty acid binding protein (FABP) per μm^2 than medium (>1.26 to <2.8 μm) or large (>2.8 μm) sized droplets. Milk-fat-globule-EFG-8 (MFG-E8) protein was more evenly distributed on small, medium and large droplets. In contrast CD36, in both cow and mouse milk, was concentrated on small droplets and absent from large droplets. Based

on these data, we postulate that CD36 possibly association with FABP may have a function in small lipid droplet secretion by localizing excessively on the small lipid droplets.

THE POTENTIAL ROLE OF MILK-FAT-GLOBULE-MEMBRANE (MFGM)
PROTEINS IN REGULATING THE SIZE OF MILK-LIPID DROPLETS

By

Hyunsu Shin

Thesis submitted to the Faculty of the Graduate School of the
University of Maryland, College Park, in partial fulfillment
of the requirements for the degree of

Master of Science

2012

Advisory Committee:

Professor Ian. H. Mather, Chair

Professor Richard Erdman

Associate Professor Brian Bequette

© Copyright by

Hyunsu Shin

2012

ACKNOWLEDGEMENTS

The completion of this thesis could not have been possible without the support and encouragement from people around me. Firstly, I would like to thank my advisor Dr. Ian Mather, for being an incredibly patient mentor. He gave me a number of great opportunities to overcome many challenges with language and limited understanding of science. His unyielding dedication and passion always inspired me whenever I encountered difficult situations. I am very grateful for the invaluable experiences I had under the guidance of Dr. Mather.

I would like to thank to my committee members Dr. Brian Bequette and Dr. Richard Erdman for their guidance of my study.

I also appreciate all past lab members, Jinling Xu, Jaekwang Jeong, and Anil Kadegowda. Anil has been like my second advisor and Jaekwang was a teacher for my life in the U.S.

I thank Diwakar Vyas for discussions regarding my studies on many occasions and for helping me. Also, my former classmates, Jason Yang, Kwon Her and Bobby Kim – they became my English tutors and very good friends, and Jungmin Choi, my other mentor.

I would like to thank the CMREC crew for always helping me to get samples and Dr. Angela Black and staff for help with animal care. I would like to thank Dr. Charles Delwiche (Dept. Cell Biology and Molecular Genetics) for use of the Beckman multi-sizer. Dr. Daniela A. Malide is especially thanked for helping me analyze the confocal micrograph data and allowing me access to the NIH imaging facilities. Dr. Iqbal Hamza's lab allowed me to use their instruments when needed, for which I am grateful. I am thankful for the care and financial support from the department and the staff of the department for all their help. I especially would like to thank my parents, sister, and You jin. Without their endless support and encouragement, I could not have endured the struggles I had while I was still trying to adapt to the graduate program. I thank you all.

TABLE OF CONTENTS

List of Tables.....	v
List of Figures.....	vi
List of Abbreviations	ix
Introduction.....	1
Materials and Methods.....	23
Materials.....	23
Methods.....	24
Milk sample processing.....	24
Sucrose gradients.....	24
Sample quantification.....	25
SDS-Polyacrylamide gel electrophoresis and Western blot.....	25
Sample preparation for immunofluorescence microscopy	26
Immunofluorescence microscopy.....	26
Fluorescence intensity analysis	28
Statistical analysis	29

Results.....	29
Objective 1).....	29
Objective 2).....	35
Objective 3).....	48
Discussion.....	70
References.....	77

LIST of TABLES

Table 1. Correlation analysis between western blot intensities and surface area, size, and fat content.....	47
--	----

LIST OF FIGURES

Fig 1. Mechanism of milk-lipid and protein secretion.....	3
Fig 2. Electron microscopy of lipid secretion and MFGM formation	7
Fig 3. Bovine milk-lipid droplet size distribution.....	9
Fig 4. Predicted topology of major proteins in the MFGM	11
Fig 5. Milk lipid droplets of BTN deficient mice.....	13
Fig 6. Milk lipid droplets of XOR deficient mice	15
Fig 7. Removal of the C-terminal portion of ADPH impairs CLD secretion.....	17
Fig 8. Proposed models for the secretion of milk-fat droplets.....	19
Fig 9. Analsis of lipid droplet fractions by SDS-PAGE.....	33
Fig 10. Modified sucrose gradient method	34
Fig 11. Micrographs of milk-lipid droplet fractions	36
Fig 12. Separation of MFGM proteins in different sized lipid droplets by SDS-PAGE	37
Fig 13. Estimation of the relative amounts of BTN in lipid droplet fractions by quantitative western blot	39
Fig 14. Estimation of the relative amounts of XOR in lipid droplet fractions by quantative western blot.....	40

Fig 15. Estimation of the relative amounts of ADPH in lipid droplet fractions by quantative western blot.....	41
Fig 16. Estimation of the relative amounts of CD36 in lipid droplet fractions by quantative western blot.....	43
Fig 17. Estimation of the relative amounts of FABP in lipid droplet fractions by quantative western blot.....	44
Fig 18. PCA of the amount fo protein to the size, surface area, and fat from the western blot data	46
Fig 19. Analysis of the distribution of BTN on bovine lipid droplets by confocal microscopy.....	50
Fig 20. Analysis of the distribution of XOR on bovine lipid droplets by confocal microscopy.....	52
Fig 21. Analysis of the distribution of ADPH on bovine lipid droplets by confocal microscopy.....	54
Fig 22. Analysis of the distribution of FABP on bovine lipid droplets by confocal microscopy.....	56
Fig 23. Analysis of the distribution of CD36 on bovine lipid droplets by confocal microscopy.....	58
Fig 24. Analysis of the distribution of BTN on mouse lipid droplets by confocal microscopy.....	60

Fig 25. Analysis of the distribution of ADPH on mouse lipid droplets by confocal microscopy.....	62
Fig 26. Analysis of the distribution of CD36 on mouse lipid droplets by confocal microscopy.....	64
Fig 27. Analysis of the distribution of MFG-E8 on mouse lipid droplets by confocal microscopy	67
Fig 28. Comparison of the amount of BTN and CD36 in small droplet and pellet fractions.....	69
Fig 29. Potential topology of MFGM proteins localization in the mammary epithelial cells	74

LIST OF ABBREVIATIONS

3D	3 dimensional
ATGL	adipose triglyceride lipase
ADPH	adipose differentiation-related protein
b	Bovine
BCA	bicinchoninic acid
	cow and mouse
BTN	butyrophilin 1a1, regardless species
CD36	cluster of differentiation 36
CLA	conjugated linoleic acid
CLDs	cytoplasmic lipid droplets
FAT	fatty acid translocase
FABP	fatty acid binding protein
FAPS	fluorescence activated particle sorting
HMWP	high molecular weight protein
Igs	Immunoglobulins
m	Mouse
MLDs	micro-lipid droplets
MFG-E8	milk fat globule-EGF factor 8 protein
MFGM	milk-fat-globule membrane

MUC1	mucin1
MS	multiple sclerosis
MOG	myelin oligodendrocyte glycoprotein
TLCK	N α -p-tosyl-L-lysine chloromethyl ketone hydrochloride
TPCK	N α -p-tosyl-L-phenylalanine chloromethyl Ketone
PSA6/7	periodic acid schiff glycoprotein 6/7
PBS	phosphate-buffered saline
PCA	principal component analysis
PM	plasma membrane
PMSF	Phenylmethyl sulfonyl fluoride
rER	rough endoplasmic reticulum
SDS	sodium dodecyl sulphate
SV	stromal vascular
TEMED	tetramethylethylenediamine
t10, c12	<i>trans</i> -10, <i>cis</i> -12
TAG	triacylglycerol
TBS	Tris-buffered saline
XOR	xanthine oxidoreductase

INTRODUCTION

Milk is composed of essential constituents for the survival of neonates that includes water, protein, lipid, carbohydrates, minerals, ions, and vitamins. Constituents vary depending upon the stage of lactation, dietary factors, breed of animal, species, and environmental conditions

There are four major secretory pathways for transferring components from mammary epithelial cells into milk: exocytosis of the proteins from secretory vesicles, secretion of lipids coated with the membrane, trans-membrane secretion of ions and water, and transcytosis of extra-alveolar proteins [1]. Most components in the aqueous phase of milk are secreted through exocytosis. Proteins, synthesized on ribosomes and folded in the rough endoplasmic reticulum (rER), are transferred to the Golgi apparatus, packaged into secretory vesicles, and secreted into milk by exocytosis [2]. In the case of extra-alveolar proteins, such as immunoglobulins (Igs), hormones, and serum albumin, these molecules, synthesized by plasma cells in the interstitial spaces or elsewhere in the body, can cross the epithelial cells from the interstitial space by transcytosis (endocytosed and transferred across the cell) [3]. However, milk lipid secretion is regulated by a mechanism unique in biology, and is the prime focus of this thesis.

The major milk lipids are triacylglycerols (TAGs), which constitute about 98% of total milk fat [4]. In the secretory pathway, micro-lipid droplets (MLDs) are released from the rER, and progressively fuse with one another to become cytoplasmic lipid droplets

(CLDs) during transport to the apical surface. The CLDs become coated with apical plasma membrane at the cell apex. Therefore, secreted milk lipid droplets are enveloped with material from the rER, including a monolayer of phospholipids and protein, and a bilayer of phospholipids and membrane proteins from the apical surface [5, 6]. This entire surface coating is termed the milk-fat-globule membrane (MFGM). (Fig 1, mechanism A and B, and pathway I and II). It is unclear if the fusion of MLDs to CLDs and transition of CLDs to the apical membrane are regulated by different mechanisms or through random processes [6]. Fusion of Golgi-derived secretory vesicles and lipid droplets under certain conditions leads to the formation of intracytoplasmic structures, which may fuse with the apical plasma membrane, followed by release of lipid droplets from the cells by exocytosis (Fig 1, mechanism C). A combination of apical and secretory-vesicle routes may be possible (Fig 1, mechanism D). Proteins, such as caseins, are transported to the Golgi apparatus, packaged into secretory vesicles, and secreted into milk by exocytosis (Fig 1, mechanism E).

A question that remains unanswered is “From where do all the lipids, which are associated with milk fat droplets, arise and how do they assemble into lipid droplets?” The formation of lipid droplets requires precursors, fatty acids and glycerol, which are acquired either from the blood stream, or by *de novo* synthesis in the mammary gland [5]. Esterification of fatty acids to the glycerol backbone requires the activity of several acyltransferases, which esterify fatty acids in the *sn*-1 and *sn*-2 positions of glycerol-3-

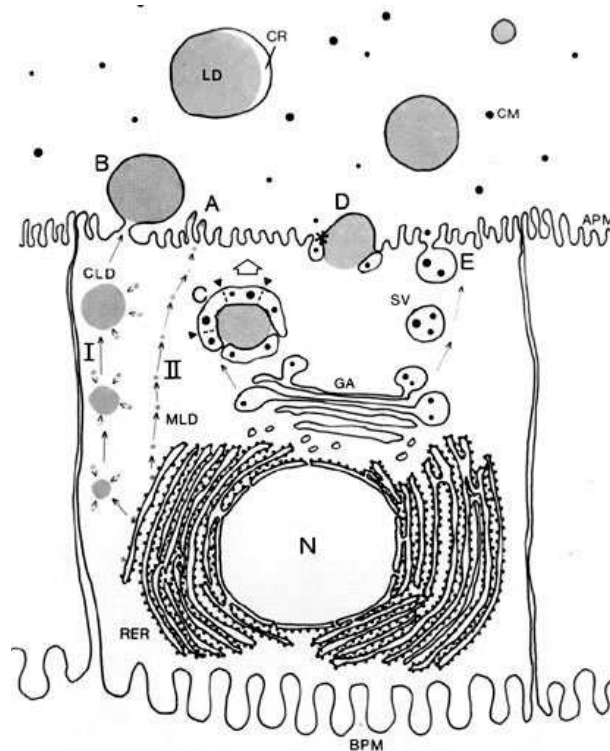


Fig 1. Mechanism of milk lipid and protein secretion Pathway I. MLDs formed in the ER fuse with each other and with larger CLDs. CLDs are transported through the cytoplasm to the apical plasma membrane, and surrounded by the membrane bilayer of the apical surface. Pathway II. MLDs are directly transported to the apical surface. Mechanism C. Intracytoplasmic structures formed from secretory vesicles, fuse with the apical plasma membrane, and the droplets are released from the cells by exocytosis. Mechanism D. A combination of secretory-vesicle and apical routes may be possible. Mechanism E. Caseins and other skim-milk proteins are secreted by exocytosis. Apical plasma membrane (APM), basal plasma membrane (BPM), cytoplasmic lipid droplet (CLD), casein micelle (CM), cytoplasmic crescent (CR), rough endoplasmic reticulum (rER), lipid droplet (LD), Golgi apparatus (GA), microplid droplet (MLD), nucleus (N), secretory vesicle (SV) [6].

phosphate (phosphatidic acid). Subsequently, the phosphate group in the *sn*-3 position is removed by a phosphohydrolase. Finally, *sn*-1,2-diacyl-*sn*-glycerol is acylated by acyltransferases [7, 8]. In a study of the intracellular movement of labeled lipid by electron microscopy autoradiographs, injection of either ^3H - glycerol or ^3H - palmitate showed that radioautographic reactions were localized to the rER one min after injection, but no radioactivity was observed in the Golgi apparatus. The latter indicates that lipid droplet formation does not require Golgi-derived secretory vesicle formation but is localized to the rER [9]. Other sources of lipid (phospholipids or cholesterol) are also associated with the rER and bilayers of the plasma membrane. Surface coat materials on CLDs are similar to the phospholipid components of rER [10]. rER resident proteins such as protein disulfide isomerase, calreticulin, and immunoglobulin binding protein are present in CLDs, which suggests the association of the rER membrane with the formation of lipid droplets [11-13]. The rER involvement in lipid droplet formation is also suggested by electron microscopy. Droplets appear to be released into the cytoplasm coated with proteins and polar lipid from the ER [12, 14]. In conclusion, lipids originate in the rER from precursors, which are obtained either from the blood stream or by *de novo* synthesis. Droplets formed in the rER are transported to the apex of the cell and coated with apical plasma membrane.

Mechanisms associated with the migration of lipid droplets towards the apical membrane are not clear but may require microtubules and other cytoskeletal elements. Both microtubules and actin-containing microfilaments are abundant in mammary

epithelial cells. Microtubules are oriented perpendicularly to the apical plasma membrane, which is possibly related to the function of guiding secretory vesicles and lipid droplets to the cell apex [15]. When microtubule assembly was reversibly blocked by the plant alkaloids colchicine and vincristine in lactating goat mammary gland, the synthesis and secretion of milk were inhibited [16]. In other studies, the concentration of fat was not significantly affected by colchicine treatment, but the concentrations of Na⁺, Cl⁻, citrate and protein were significantly increased, while K⁺ and lactose decreased [17]. The uptake of amino acids from the blood stream also decreased, which reduced milk protein yield and potentially had secondary effects on lipid secretion by affecting general cell metabolism [17]. In another study, infusion of colchicine into the lactating goat mammary glands caused an increase in milk lipid content and the diameter of CLDs. However, phospholipid content decreased, implying that colchicine did not affect milk lipid synthesis *per se*, but milk-lipid secretion, causing the accumulation of large lipid droplets in the cell [18]. By contrast, incubation of ewe and rabbit mammary tissue explants with colchicine did not affect lipid secretion. Following incubation with colchicine, addition of prolactin stimulated lipid secretion, which suggests that microtubules are not involved in lipid secretion [19]. Thus, given these conflicting results, it is not clear whether microtubules play a specific role in milk lipid secretion.

In the case of microfilaments, skeletal muscle actin and homologous actin-binding protein, as well as a high molecular weight protein (HMWP) supposedly analogous to either clathrin, or cortactin binding protein 1, are expressed more highly in

milk secreting cells compared to contractile myoepithelial cells [20, 21]. When cytochalasin B, a microfilament altering drug, was infused into the lactating guinea pig mammary gland, either lactose synthesis in the Golgi apparatus or secretion from the apical plasma membrane, or both, were inhibited, suggesting that microfilaments are associated with the secretory pathway during lactation [21]. Whether microfilaments are involved in lipid droplet secretion is not clear. Microfilaments are not detected on the surface of lipid globules and luminal areas of budding lipid droplets by immunofluorescence microscopy [22]. However, proteomic analysis has shown that actin, actin binding proteins, and the small GTP-binding protein RhoA essential for secretory function and actin remodeling, are constituents of human MFGM [23]. Whether these components play a role in milk-lipid secretion via microfilaments has not been firmly established.

There is some evidence that interaction between MFGM proteins is involved in milk lipid droplet secretion. According to electron micrographs, paracrystalline protein structures, with a lattice constant of 20nm, form between the lipid bilayer and droplet surface. This protein coat appears to partly consist of BTN and XOR [24]. These micrographs suggest that both integral and cytosolic proteins are concentrated into a regularly ordered structure with hexagonal symmetry, which may be necessary for lipid droplet secretion (Fig 2a). The outer layer of the MFGM is derived from the apical plasma membrane as shown by immunocytochemical staining for MUC1 [25] and BTN [26] (Fig 2b). During the process of lipid droplet secretion, the TAG core is separated

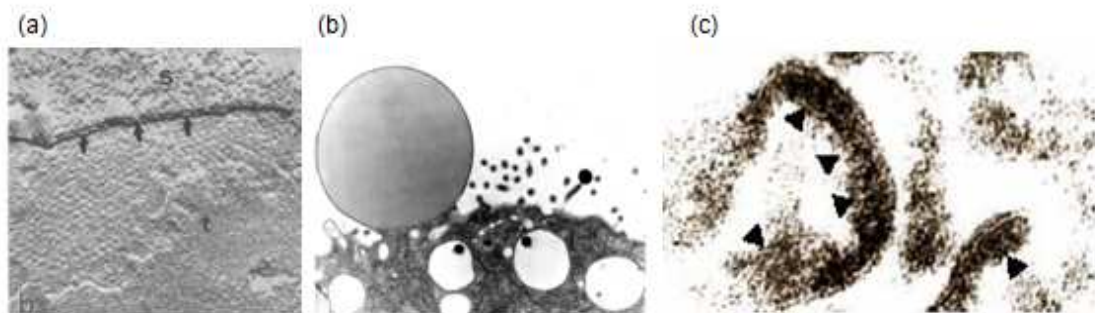
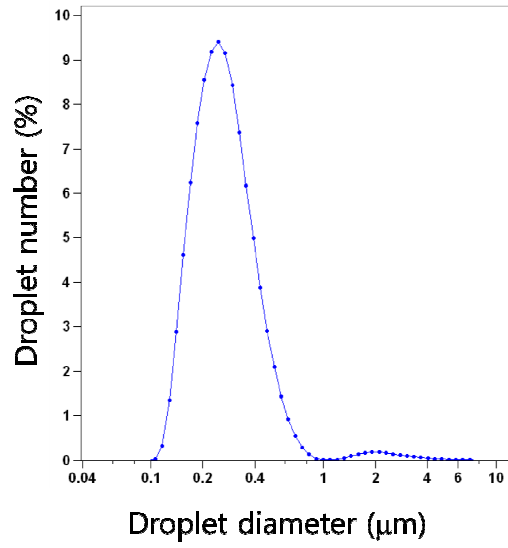


Fig 2. Electron microscopy of lipid secretion and MFGM formation. (a) Paracrystalline structure on the surface of the TAG core (inner surface of MFGM) s, outer surface, t, surface of TAG core [27]. (b) Budding lipid droplet from surface of mammary cell. (Mather, I. H., unpublished data) (c) Electron micrograph of MFGM. Arrowhead, coated inner face of membrane [28].

from the outer plasma membrane (PM) bilayer by the protein coat discussed above, which is approximately 10-20nm in thickness and appears as electron-dense material in electron micrographs of isolated membrane [24, 28] (Fig 2c). These micrographs suggest that the association of MFGM proteins in this coat structure may be required for lipid droplet secretion.

The focus of this thesis is the potential relationship between the size of milk lipid droplets and interactions between MFGM proteins. The size of lipid droplets in milk varies among species, ranging from $< 0.2\mu\text{m}$ to $> 8\mu\text{m}$ [29]. Distributional differences based on lipid droplet size indicate that the majority of the fat volume in bovine milk is associated with relatively large globules (about 90%, average $3.5\mu\text{m}$), but globules $< 1\mu\text{m}$ in diameter comprise the majority (about 80 to 90%, average $0.4\mu\text{m}$) of total droplet number (Fig 3a, 3b) [29, 30]. Attaie and Richter [31] reported that the mean diameter of milk lipid droplets is $3.51\mu\text{m}$ and 90% of lipid droplets are less than $5.21\mu\text{m}$, in contrast to caprine milk droplets which are $2.76\mu\text{m}$ in mean diameter and 90% of the lipid droplets are less than $6.42\mu\text{m}$. The average diameter of human milk lipid droplets is smaller, ranging from $2.2\mu\text{m}$ at the beginning of lactation to $2.7\mu\text{m}$ after 40 days of lactation [32]. Chung et al. [33] showed that treatment of stromal vascular (SV) cells with *trans*-10, *cis*-12 (t10,c12) conjugated linoleic acid (CLA) caused an increase in lipolytic activity and a change in morphology (smaller droplets than control). Such morphological changes were also observed in milk lipid droplets following treatment of lactating mice with t10,c12 CLA (Unpublished, Kadegowda, A. and Mather, I.H.).

a. Droplet number (%)



b. Droplet volume (%)

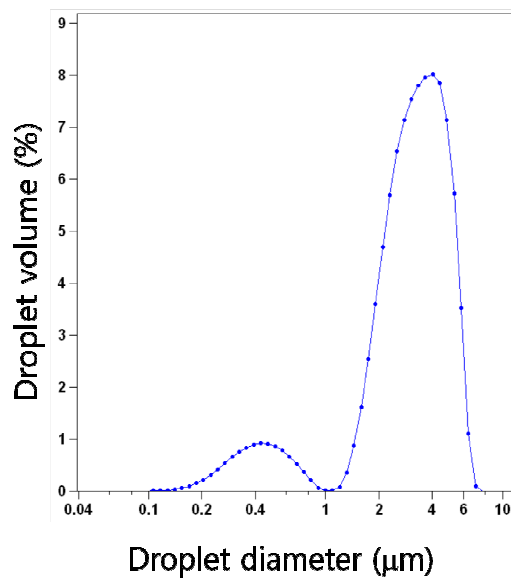


Fig 3. Bovine milk lipid droplet size distribution Size distribution according to a) number (%), b) volume (%) [29]

In order to frame the underlying hypothesis of this study, the major MFGM proteins and their functions are discussed in succeeding sections.

Based on the features and interactions of each MFGM protein and the lactation phenotypes of mice with disrupted genes, milk lipid droplet size is presumed to be regulated by MFGM proteins during secretion. Several major MFGM proteins have been studied extensively to identify their function in secretion, and (/or) internal or peripheral trafficking of lipid droplets. These proteins are localized in the MFGM in different topologies, reflecting their intracellular origins. Thus, some trans-membrane proteins are from the apical plasma membrane and may bind to other trans-membrane proteins or to proteins from the cytoplasm that are located within the space between the TAG core and the bilayer. Other droplet-associated proteins may be from the rER. Periodic acid Schiff glycoprotein 6/7 (PAS 6/7) is localized on the outer surface (exoplasmic) of the membrane bilayer [34]. BTN, MUC1, and CD36 are examples of trans-membrane proteins [25, 35]. XOR and FABP bind to BTN and CD36, respectively [36, 37]. Adipophilin (ADPH) is localized in the intra-space between the bi-layer and mono-layer membrane of the lipid droplet and potentially binds to a complex of BTN and XOR [35] (Fig 4).

MUC1 is a type I glycoprotein that is expressed in most simple secretory cells. Prominent structures in MUC1 are multiple tandem repeats in the exoplasmic domain and a short cytoplasmic tail [27]. MUC1 may protect the cell surface from physical damage, play a role in epithelial organogenesis, and promote tumor progression [38].

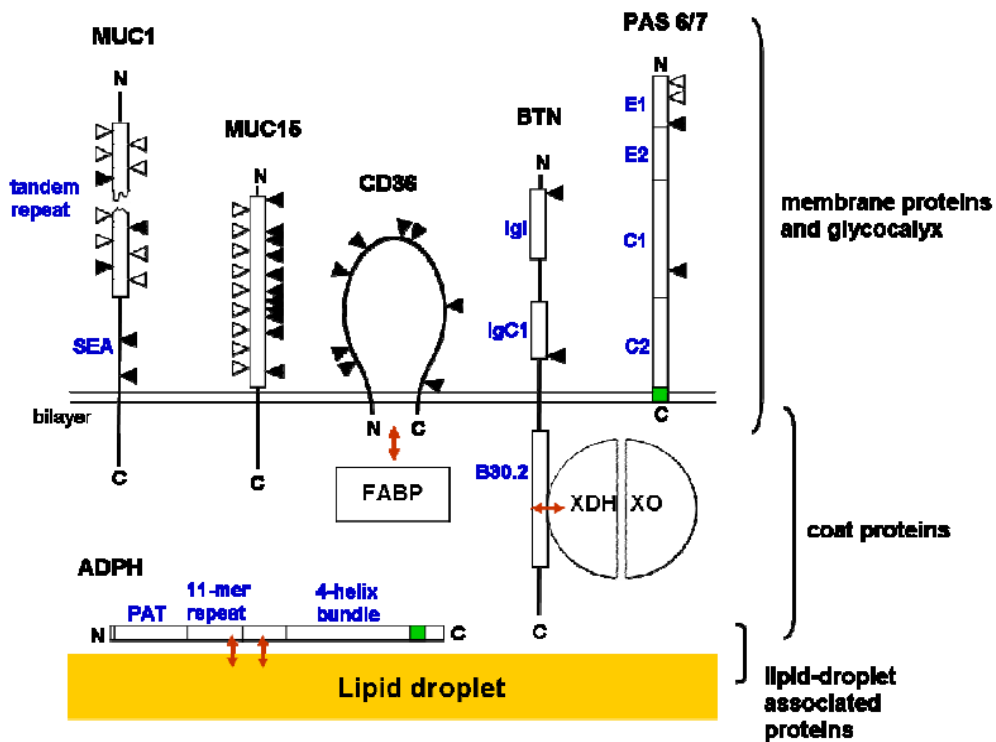
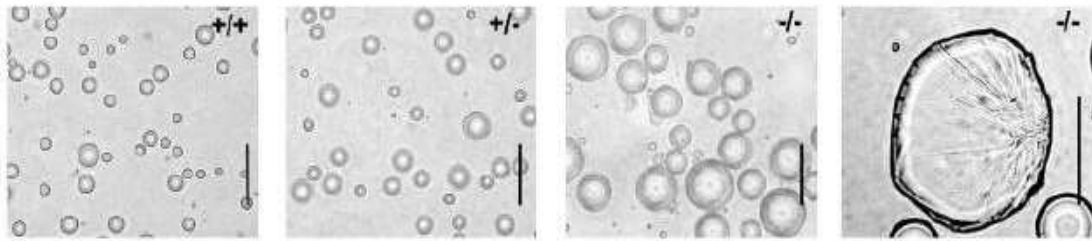


Fig. 4. Predicted topology of major proteins in the MFGM. Integral proteins include MUC1, CD36, and BTN. MUC1 has tandem repeats in the exoplasmic domain and a short cytoplasmic tail. BTN is a member of the immunoglobulin superfamily and comprises two immunoglobulin-like domains (Igl and IgC1) in the exoplasmic area, and a B30.2 domain and tail in the cytoplasmic area. XOR and ADPH are located between the bilayer and mono-layer membranes. These proteins are potentially associated with the cytoplasmic face of MFGM. CD36 co-localizes with FABP [39].

MUC1 null mice appear healthy and fertile, and lactation appears to be normal, suggesting that MUC1 is not involved in milk secretion [38].

BTN is a major MFGM protein in some species that is abundant in the apical membrane of secretory epithelial cells, but not in other mammary cell types such as myoepithelial cells, adipocytes, and endothelial cells. Most of the proteins in the BTN gene family are type I integral membrane proteins. BTN1A1, BTN2A1 to 3 and BTN3A1 to 3 are expressed in various tissues, but BTN1A1 is the only BTN that is highly expressed in lactating mammary tissue [40]. The exoplasmic domain comprises two Ig folds that comprise an intermediate type (Igl), which is located near the N terminus, and a constant type (IgC1), which is close to the membrane [41]. These Ig folds function in suppressing T-cell activation [42]. The cytoplasmic domain comprises a B30.2 domain which binds to XOR and a C-terminal tail [36]. According to amino acid sequence alignments, the secondary structures of B30.2 domains have a conserved binding interface [43]. Active immunization with BTN triggers an autoimmune response, because of structural similarities between the Igl domain of BTN and the IgV fold of myelin oligodendrocyte glycoprotein (MOG), a brain-specific auto-antigen [44]. Such autoimmune responses may lead to multiple sclerosis (MS) –like pathologies. BTN appears to have multiple functions, including immune responses (immunosuppression) and milk lipid droplet secretion. *Btn*^{-/-} mice have a lactation phenotype, in which lipid droplets accumulate in the cytoplasm, and lipid secretion is defective. Secreted lipid droplets are also larger and unstable compared with those of wild type mice [45] (Fig 5).

(i)



(ii)

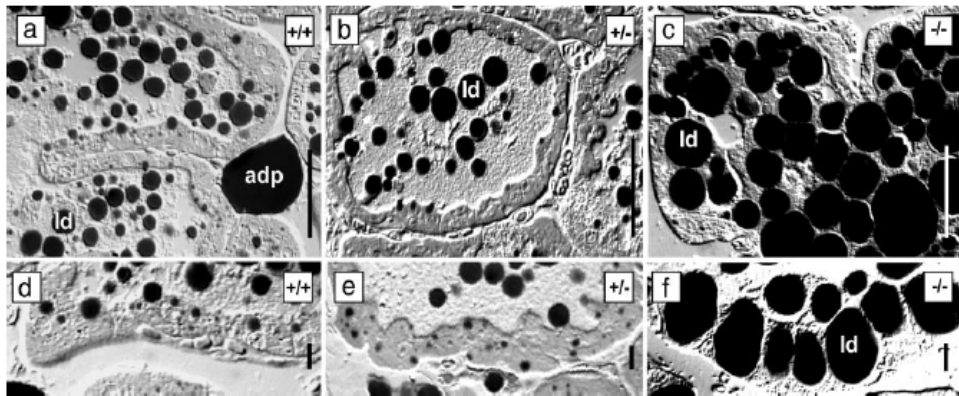


Fig 5. Milk lipid droplets of BTN deficient mice. (i) lipid droplet size differences among *Btn1a1*^{+/+}, *Btn1a1*^{+/-} and *Btn1a1*^{-/-} mice. (ii) accumulation of lipid droplets within lactating mammary tissue from *Btn1a1*^{+/+}, *Btn1a1*^{+/-} and *Btn1a1*^{-/-} mice [45].

Thus, according to the analysis of *Btn*^{-/-} mice, disruption of the *Btn* gene impairs the regulation of milk-lipid droplet secretion and size.

XOR is expressed in most cell types and especially at high levels in mammary epithelial cells during lactation. XOR is a homodimer of a 150,000 Da protein. Each subunit has four redox centers, comprising a molybdopterin cofactor (Mo-Co), one FAD molecule, and two Fe₂S₂ clusters. The main function of XOR in most cells is in purine metabolism and innate immunity [46]. XOR may have a crucial role in milk-fat globule secretion because its expression begins to increase in mid-pregnancy and is sharply increased at the onset of lactation, binding to the B30.2 domain [36]. In a recent study, ablation of *Cidea*, a transcriptional cofactor for C/EBPβ, down regulated expression of XOR, which impaired secretion and regulation of droplet size; small lipid droplets accumulated in the cytoplasm [47]. In addition, XOR-deficient mice (*Xdh*^{-/+}) have a similar lactation phenotype as BTN disrupted mice [48] (Fig 6). Results from disruption of *Cidea* and *Xdh* are contradictory, but functions of XOR in milk lipid size regulation and secretion are evident. Furthermore, cytosolic XOR is redirected to the apical plasma membrane during lactation by binding to BTN (Jeong, J.K., Kadegowda, A.K., and Mather, I.H., unpublished). The similar phenotypes from disruption studies of the two genes (BTN and XOR) and physical interaction between the two proteins suggests potential roles in droplet size regulation and secretion.

CD36 is a 76 to 78kDa integral protein [6]. The expression of CD36 is high in cells such as differentiated adipocytes and mammary secretory epithelial cells, which

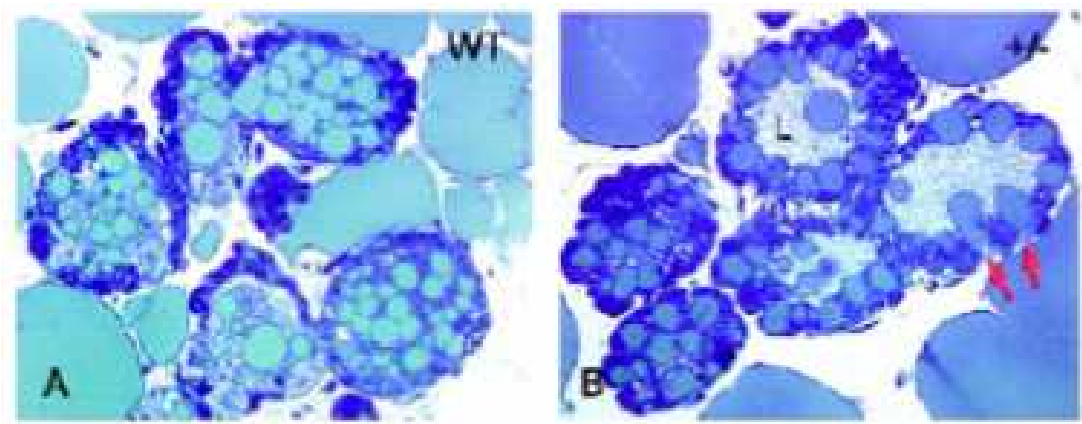


Fig 6. Milk lipid droplets of XOR deficient mice. A. $Xdh^{+/+}$, B. $Xdh^{+/-}$ milk lipid droplets accumulate in lactating mammary tissue (red arrows) (similar to $Btn1a1^{-/-}$ mice) [48].

store and secrete TAGs [49]. CD36 is a fatty acid translocase (FAT) which functions in transporting long chain fatty acids from the cell exterior to the interior, and is present at the plasma membrane. CD36 is mainly concentrated on the apical plasma membrane and basal/lateral surfaces of secretory epithelial cells [7, 49]. Additionally, interaction between CD36 and FABP may affect the growth of the mammary epithelium [37]. However, no functions for either CD36 or FABP in lipid secretion have been established.

Adipophilin (ADPH) is a PAT family protein (perilipin, adipophilin, and TIP47), sharing a homologous sequence termed the PAT domain. These PAT family proteins are potentially implicated in intracellular lipid metabolism, but their exact function is unclear. ADPH is also possibly involved in lipid droplet formation during transit to the apical region by regulating lipase activities or secretion by associating with either the bilayer membrane directly or by functioning in other MFGM proteins in mammary epithelial cells [50]. The concurrent increase of ADPH mRNA and protein levels with CLD accumulation during late pregnancy as well as co-localization with XOR and BTN suggest that ADPH may play a role in regulating lipid droplet secretion [51]. The N- and C- termini of ADPH have different functions. A recent study has shown that over-expression of ADPH lacking the C-terminus impaired lipid secretion [50]. Thus, secretion of lipid droplets may be regulated by interaction of ADPH with the phospholipid bilayer through a C-terminal membrane binding helical structure (Fig 7). On the other hand, the structure of cytoplasmic lipid droplets is stabilized through the N-terminus of ADPH [50]. A recent study suggests that ADPH-deficiency impairs the accumulation of CLDs and interferes



GFP-ADPH(fl)-VSV **GFP-ADPH(1-220)-VSV**

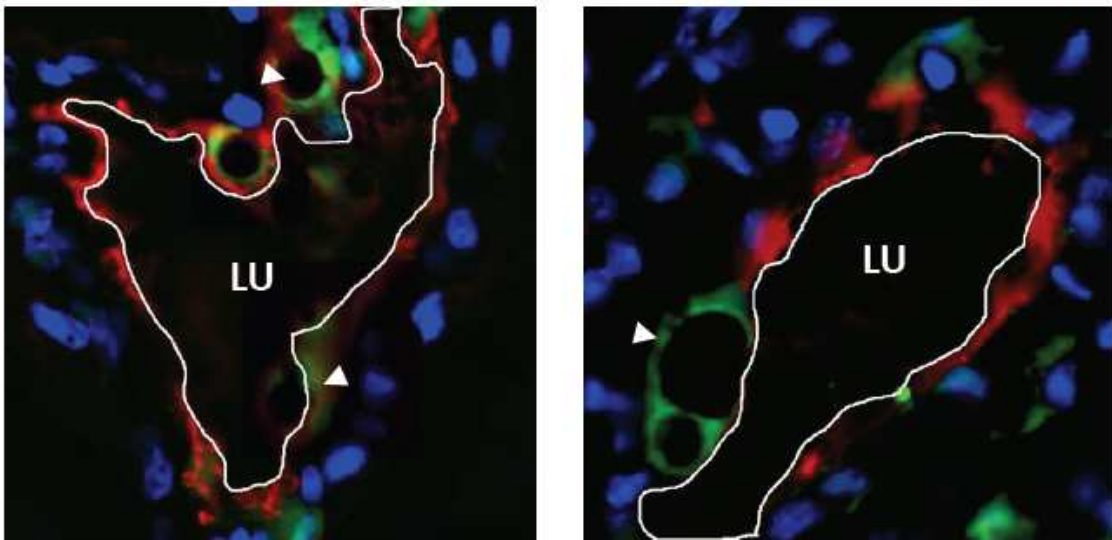


Fig 7. Removal of the C-terminal portion of ADPH impairs CLD secretion. Overexpression of the N-terminus of ADPH via viral vector transduction impairs CLD secretion (right) compared with transduction of full length ADPH (left) [50]

with alveolar maturation and lactation by disrupting TAG homeostasis [52].

PAS6/7 is a bovine homolog of mouse milk fat globule-EGF factor 8 protein (MFG-E8) [6]. MFG-E8 may play an important role in the recognition and engulfment of apoptotic epithelial cells by binding to phosphatidylserine (PS) in involuting mammary glands [53]. However, there is no clear function for MFG-E8 in lipid droplet secretion.

In conclusion, how the size of milk lipid droplets is regulated is not clear. Analysis of the phenotypes of *Btn*^{-/-} and *Xdh*^{+/-} mice suggests that BTN and XOR are required for lipid secretion. Furthermore, these MFGM proteins interact with each other, further suggesting a role for both proteins in secretion. In addition, CD36 interacts with FABP, although the functional significance of this interaction is unknown. The underlying hypothesis of this work is that interaction between MFGM proteins may play an important role in the regulation of droplet size.

Several models have been proposed to explain the mechanism of milk lipid secretion. In the first proposed model, Mather and Keenan suggested that BTN localizes in the apical membrane and interacts with XOR (Fig 8 a.) [7]. The CLDs are coated with XOR as droplets transit to the apical membrane, and then XOR on the CLDs interacts with BTN through the B30.2 domain in the C-terminus of BTN [36]. Once these proteins interact, the lipid droplet pushes against the apical plasma membrane of the mammary epithelium and finally pinches off from the cell coated with an outer bilayer membrane. The 10 to 20- nm thick protein coat between droplets and the cytoplasmic side of the membrane seen in electron micrographs [54] and discussed

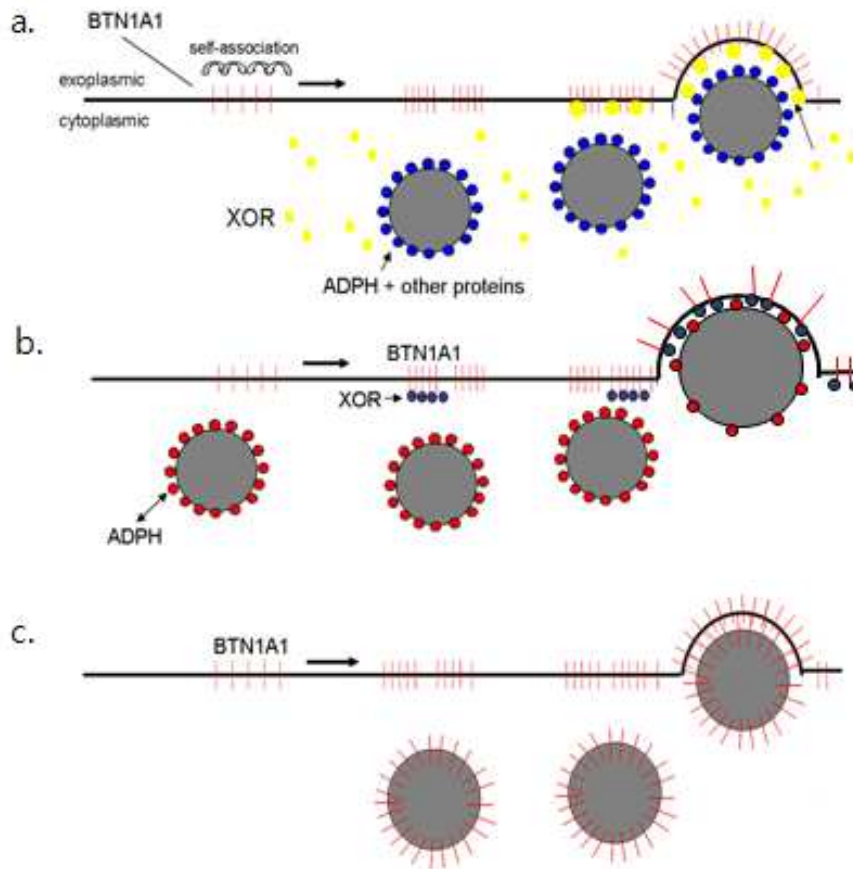


Fig. 8 Proposed models for the secretion of milk-fat droplets a. BTN in the apical membrane interacts with XOR either in the apical membrane or on the surface of lipid droplets [7], b. XOR interacts with BTN in the apical membrane and ADPH on the surface of lipid droplet [50], c. Lipid secretion is regulated by interaction between BTN located both in the apical membrane and the surface of the lipid droplets [55].

above is assumed to partly consist of XOR and the cytoplasmic tail of BTN. In a second proposed model, XOR interacts with BTN and also with ADPH, which associates with the droplet directly. As the complex is formed, the droplets are pinched off from the cell (Fig 8 b.) [51]. In a third model, Robenek et. al. [55] proposed that BTN in the MFGM is concentrated both on the droplet surface and the apical membrane. Milk lipid droplet secretion is regulated through interactions between BTN on the droplets and BTN in the membrane. In this model, XOR and ADPH have no function in the secretion of lipid droplets. This latter proposal is based on the results of freeze-fracture immunocytochemistry, which showed that BTN was abundant on the droplet and bilayer membrane. Thus, in this model, milk lipid secretion is entirely regulated by interactions between BTN on the droplet and apical plasma membrane (Fig 8 c.).

Even though the mechanism of milk lipid droplet secretion is controversial, evidence from gene targeting studies supports the first proposed mechanism. Ablation of the BTN gene causes defects in the formation, secretion, and size regulation of lipid droplets [45]. Additionally, XOR disrupted mice (*Xdh+/-*) have a similar phenotype to that of *Btn1a1-/-* mice [48]. Several studies also suggest that these MFGM proteins co-localize and function together [36, 37, 48].

Then, how is droplet size regulated? Besides the secretion mechanism, little work has been conducted on the regulation of droplet size. One possible mechanism for regulating lipid droplet size within the cell is during transition from MLDs to CLDs. This process may be regulated by differences in lipid composition [29]. The proportion of

phospholipids in total MFGM lipids is higher in the MFGM of large lipid droplets than in that of small lipid droplets. In addition, the phospholipids in small lipid droplets contain more saturated fatty acids than large lipid droplets. The compositional differences of fatty acids between large (composed of more short chain fatty acids) and small globules (composed of less short chain fatty acids) may contribute to CLD' size by regulating the fusion of MLDs [29]. Adipose triglyceride lipase (ATGL) activity is one of the factors that regulates droplet size [51]. During transport from basal to apical regions, ADPH coats lipid droplets, and therefore blocks access to ATGL on the droplet surface, such that the size increases as lipase activity is inhibited. Another possible mechanism for regulating lipid droplet size is associated with proteins that interact during the secretion process. BTN as an integral protein may function as a scaffold linking the outer membrane bilayer to XOR and potentially interacts with other MFGM proteins, such as ADPH, on the droplet surface [45, 48, 51]. In addition, CD36 interacts with FABP. If these interactions contribute to the regulation of droplet size, then the MFGMs of small lipid droplets may have a different protein composition from those of large lipid droplets.

Therefore, we hypothesize that a complex, which regulates the size of lipid droplets, is formed between BTN, XOR and other proteins. Although there are various possibilities, we propose that small droplets are secreted immediately when they arrive at the apical surface, provided that sufficient amounts of BTN/XOR and other proteins are available. If such proteins are limiting in amount, the droplets are postulated to grow until sufficient protein has accumulated to trigger their release from the cell. To test the

possibility that the relative amount of certain MFGM proteins correlates with the size of milk lipid droplets, the following aims were completed:

- 1) To devise a method for separating small, medium, and large droplets from bovine milk.
- 2) To determine whether the relative amount of specific MFGM proteins correlates with milk fat globule size by measuring the amount of bovine XOR, CD36, BTN, ADPH, and FABP in fractions of small, medium and large lipid droplets by quantitative western blot.
- 3) To confirm differences in protein distribution in lipid droplets of different size by measuring the relative amounts of specific MFGM proteins in small, medium and large lipid droplets by confocal microscopy.

Materials and Methods

Materials

Tris hydroxymethyl amino methane (Tris), sodium dodecyl sulphate (SDS), ammonium persulphate, N,N,N',N' tetramethylethylenediamine (TEMED), goat anti-(rabbit-IgG) conjugated to horse-radish peroxidase, nitrocellulose, coomassie brilliant blue R-250, acrylamide, N,N' methylenebisacrylamide, and Triton X-100 were obtained from Bio-Rad Laboratories (Hercules, CA). N-p-tosyl-L-phenylalanine chloromethyl ketone (TPCK), N α -p-tosyl-L-lysine chloromethyl ketone hydrochloride (TLCK), DL dithiothreitol (DTT), aprotinin, sucrose and glycerol were obtained from Sigma-Aldrich Inc. (St.Louis, MO). Bicinchoninic acid (BCA) protein assay reagents were from Pierce Chemical Company (Rockford, IL). ECL™ western blotting detection reagents were obtained from Amersham Life Sciences (Pittsburgh, PA). Bovine serum albumin (BSA) and phenylmethyl sulfonyl fluoride (PMSF) were from Calbiochem (CA). Rabbit polyclonal antibody to CD36 was obtained from Abnova (Jhongli, Taiwan). Goat anti - (rabbit IgG-Alexa488), rabbit anti - (goat IgG- Alexa 546), BODIPY 665/676 (Eugene, OR), Nile red, and ProLong Gold antifade reagent were obtained from Invitrogen (Carlsbad, CA). Poly-L-lysine coverslips were obtained from BD Biosciences (Bedford, MA) and superfrost plus micro slides were from VWR (West Chester, PA).

Methods

Milk sample processing

Milk from five Holstein dairy cows at the Central Maryland Research and Education Center (CMREC), Clarksville, was collected at the regular morning milking. Milk (250 ml) was centrifuged at 10,000 x *g* in a Sorvall RC-5 superspeed centrifuge using a Sorvall GSA rotor at room temperature. The floating layer of fat was washed once with PBS, pH 7.4 (137mM NaCl, 2.7mM KCl, 10mM Na₂HPO₄, and 2mM KH₂PO₄) and the mixture again centrifuged at 10,000 x *g*. Casein micelles were removed by washing at 10,000 x *g* with PBS containing 1mM EDTA and fractionated by sucrose gradients.

Sucrose gradients

Washed cream samples, prepared as above, were fractionated by centrifugation on sucrose gradients. Washed cream was mixed with 2 M sucrose in PBS to a final sucrose concentration of 1.5 M. The whole cream mixture was placed at the bottom of 50ml centrifuge tubes and overlain successively with 1.5 M, 1.0 M and 0.25 M sucrose. The samples were then centrifuged for 10 min at 1,000 x *g* at room temperature. The milk fat globular size distribution of each fractionated sample was measured with the Beckman multi-sizer (Multisizer™ 3 Coulter counter®, Beckman coulter, Inc. Brea CA). The size, surface area, and count of particles were measured dependent on measurable changes in electrical resistance from nonconductive particles suspended in an electrolyte, as a principle of electrical sensing zone method in Beckman multi-sizer.

Sample quantification

The raw data for each protein have to be related to a property of the droplets. Therefore, the amount of each specific protein was related to total MFGM protein, total neutral lipid and total surface area. The total protein concentration of each sample was measured by BCA assay [56]. Neutral lipid was extracted with hexane and estimated by gravimetric analysis [57]. The total surface area of the lipid droplets was measured with a Beckmann multi-sizer. Samples were stored with protease inhibitors at -20 °C (0.25mM TLCK, 0.25mM TPCK, 1.25mM PMSF, 0.2 mM ϵ -amino-n-caproic acid and 0.15 units of aprotinin).

SDS-Polyacrylamide gel electrophoresis and Western blot analysis

Samples were prepared for electrophoresis by heating to 95 °C in SDS-PAGE buffer (50mM Tris-HCl, pH 6.8, 10% glycerol, 2% SDS, 0.05% bromophenol blue, and 150mM DTT) for 3 min, and separated in 10% (w/v) polyacrylamide gels at a constant current of 80 mA for 3h [58].

For Western blotting, separated proteins were transferred onto a nitrocellulose membrane according to the method of Towbin et al. [59]. The membranes were blocked with 5% non-fat dried milk in high-salt TBS (20 mM Tris, pH 7.4, and 0.5M NaCl), overnight. After overnight incubation, the membranes were washed three times, for 15 min each time, with high-salt TBS. Membranes were incubated with primary antibodies to BTN, XOR, ADPH, CD36, or FABP in 2.5% non-fat dried milk (high-salt TBS for 2h). After primary antibody incubation, the membranes were washed with high-salt TBS

three times for 15 min each time and then incubated with goat-anti-rabbit IgG conjugated to horse radish-peroxidase in 2.5% non-fat dried milk in TBS for 1h. The membranes were again washed three times with high salt TBS and the bound peroxide was detected using the Amersham Western blotting kit. Band intensities were quantified using the Quantity One software program (Bio-Rad).

Sample preparation for immunofluorescence microscopy

Milk from three Holstein cows in peak lactation from the dairy herd at CMREC, Clarksville was collected at the regular morning milking. Milk (250 ml) was centrifuged at 10,000 $\times g$ in a Sorvall RC-5 superspeed centrifuge using a GSA rotor at room temperature. The floating layer of fat was washed once with PBS (250 ml) at 10,000 $\times g$ and each washed suspension adjusted to an absorbance of 2.0, at 600 nm.

Mouse milk was collected from CD1 day 10 lactating mice. Mice were anesthetized by intraperitoneal injection of avertin at a dosage of 125 to 250 mg/kg body weight, and injected with 0.21 I.U. of oxytocin in physiological saline. After injection, mouse milk was collected via vacuum pump into capillary tubes. Mouse cream was washed and collected by centrifugation at 10,000 $\times g$ in TBS, and adjusted to an absorbance of 2.0 at 600 nm. All procedures for animal care and animal protocols were approved by the Institutional Animal Care and Use Committee (IACUC) of the University of Maryland, College Park (given protocol number from University is R-09-46).

Immunofluorescence microscopy

Washed milk lipid droplets were fixed with 4% paraformaldehyde in 125 mM HEPES, pH 7.35 and placed onto poly-L-lysine coated cover-slips (for mouse cream) or

Super-frost cover-slides (for bovine cream) for 10 min. After incubation with paraformaldehyde, droplets were quenched by washing three times with 50mM NH₄Cl in TBS. If the MFGM protein epitope was located at the internal (cytoplasmic) site, the droplets were permeabilized with surfactant, *viz-* lipid droplets were permeabilized with 0.2% saponin for 30 min for bBTN and bXOR, 0.5% saponin for 30 min for bFABP, 0.02% digitonin for 30 min for bADPH and mADPH [60], and 0.2% Triton-X 100 /TBS for 10 min for mBTN. After permeabilization, these samples were blocked with 1% BSA for 30 min. For external (exoplasmic) epitopes, droplets were directly blocked by 1% BSA in TBS for 30 min. Cover slips or cover slides were washed with TBS three times, and then incubated with primary antibodies diluted 1 to 50-fold in 1% BSA (BTN, XOR, ADPH, CD36, MFG-E8 and FABP) for 1h at room temperature. Droplets were washed with TBS three times, and then incubated with secondary antibody diluted 1 to 200-fold; goat anti-rabbit IgG Alexa 488, or rabbit anti-goat IgG Alexa 546 in the case of the MFG-E8 antibody and 10µm BODIPY-650 in blocking solution for 1 h at room temperature. Incubated droplets were washed with TBS three times, and then sealed with ProLong antifade reagent by solidification. Micrographs were recorded using excitation wavelengths at 488nm and emission between 500-530nm for Alexa 488, at 546nm and emission between 556-573nm for Alexa 546, and excitation wavelength at 665nm and emission at 676-715nm for BODIPY 665. In order to make a 3 dimensional structure reconstruction, samples were scanned in z at a thickness of 0.42µm, for a total thickness ranging from 7.3 to 17.6µm. Ten micrographs for each protein (three cows and three mice) were recorded (total 30 of micrographs for each protein), using the

same confocal setting, under conditions with no evidence of optical saturation in any of the droplets.

Fluorescence intensity analysis

Three bovine and three mouse milk samples were obtained for immunofluorescence staining with MFGM proteins. A series of high resolution images (100nm/pixel) along the z-axis were collected throughout the depth of the sample and reconstructed as three-dimensional images using Imaris 7.4 (Bitplane, Zurich, Switzerland) software. The fluorescence intensities of each protein covering the lipid droplets (green channel) over each individual lipid droplet (red channel) were calculated in 3D using the Imaris Surpass module: the lipid droplets (red channel) were segmented as isosurfaces using an automatic intensity thresholding algorithm of the software and user-edited by additional splitting when the automatic creation was found not to be fully accurate. The size (area) of the segmented lipid droplets as well as fluorescence intensity (mean) of the green channel over these objects was software computed and all data were exported as MS excel files for further analysis. Due to the fluorescence intensities are slide condition dependent, intensities from each animal within the same protein were normalized. The mean intensity from different animals for each protein was adjusted based upon the highest mean value among the three animals. Outliers were cut-off when a value was over three standard deviations from the mean of adjusted intensities. Based on these data, scatter plots were obtained for statistical analysis.

Statistical analysis

The differences in the levels of different proteins measured by Western blot in

different sized lipid droplets were analyzed for statistical significance by ANOVA with a post hoc Tukey's test. Values were considered significant at a *P*-value of 0.05. Principal component analysis (PCA) and correlation analysis were performed to determine the inter-relationship between the lipid droplets and the MFGM proteins using SAS (SAS 9.2 SAS Institute Inc. Cary, NC). ANOVA with a post hoc Tukey's test (pairwise) was used for statistical analysis of intensity data from immunofluorescent images after categorization of lipid droplets according to size (bovine, 5 categories; mouse, 6 categories).

Results

Objective 1)

Rationale

MFGM proteins are presumed to play an important role in the current three models of milk lipid secretion. Considering the results from MFGM gene disruption studies, we hypothesized that the regulation of lipid droplet size is dependent upon a concentration distribution of MFGM proteins and their interactions. In unpublished work (Jacob, J., Jeong, J., and Mather, I.H.), differences in MFGM protein amounts were noted in different species as well as comparative differences in droplet size, suggesting a potential role for MFGM proteins in regulating lipid droplet size. Not only MFGM

protein localization itself, but also the interactions between MFGM proteins may affect the secretion and the size of milk lipid droplets, since there is evidence of complex formation between MFGM proteins. Several different interactions between MFGM proteins have been identified, including interaction between BTN and XOR through the B30.2 domain of BTN [36], interaction of ADPH with BTN and XOR through the formation of disulphide bonds [6], and binding of FABP to CD36 [37]. As a working hypothesis, we propose that the ratio of MFGM proteins affects the ultimate size of the secreted droplets. For example, species such as the mouse, which express low amounts of BTN in the MFGM, might be expected to secrete larger lipid droplets, because the scaffold complex between BTN and XOR will be less abundant. If this is the case the amount of BTN in droplets should be inversely correlated with their size. To test this possibility, we fractionated lipid droplets according to their size and measured the amount of specific MFGM proteins in each fraction.

Development of method for fractionating lipid droplets according to size

In order to determine whether the amount of specific MFGM proteins correlates with the volume or diameter of lipid droplets, a method was required to fractionate milk lipid globules according to size. Several methods were available to achieve this aim. The first well used method is based on the application of centrifugal force, to separate droplets according to density [61]. However, successive centrifugations may cause disruption of the globule membrane structure. A second method is unit gravity separation: a density-based separation technique utilizing the varying degrees of

gravitational effects on lipid globules [62]. A third method is membrane microfiltration, which separates the fat globules by using special ceramic microfiltration membranes [63].

1) Gravity separation

The gravity separation method was adopted as a first separation trial. Whole milk was stored at 4°C for 6 h, and the first floating fraction was collected as a sample of large lipid droplets, and a second floating fraction was later collected as a sample of small lipid droplets after overnight stay at 4°C. The limitation of this method was incomplete separation results (data not shown). Thus, samples from 6 h and overnight were not different in size.

2) Gravity separation in sucrose gradients of whole milk

In an attempt to improve the limitation of gravity separation, the whole milk sample in 10% sucrose was placed under a layer of PBS buffer and the droplets allowed to separate under gravity over varying time periods (6 h, 12 h, and 24 h). After separation, the bottom layer as a small droplet fraction and the floating layer was collected as a large droplet fraction. The diameter of the droplets in each fraction was measured with a Beckmann multi-sizer. The droplets in each fraction were well separated into large and small fractions by using the sucrose gradient. However, the membrane proteins were degraded because of the extensive time required for separation at room temperature (data not shown).

3) Sucrose gradient separation by centrifugation

In order to solve the protein degradation problem, the separation time in sucrose gradients by centrifugation was reduced and further sucrose layers were added to enhance separation. Whole milk in 2 M sucrose was placed at the bottom of the tube and overlain successively with 1.5 M and 0.25 M sucrose. The samples were centrifuged for 10 min at 1,000 x *g* at room temperature. Through this method, the separation time and protein degradation were reduced and the separation improved. However, a limitation of this method is that samples are contaminated with casein micelles, especially in the bottom fraction (Fig 9a).

4) Modified sucrose gradient separation

Casein micelle contamination was minimized by an additional washing step for 15 min at room temperature. This step was repeated one more time before setting up a modified sucrose gradient (1.5 M sucrose with washed cream, 1.5 M, 1 M, and 0.25 M) at room temperature. Each fraction was then collected and washed with 1mM EDTA in PBS at 10,000 x *g* for 15 min at room temperature (Fig 10a). Casein micelle contamination was significantly reduced (Fig 9b). This method was used in all further experiments.

Analysis of the MFGM proteins from sized lipid droplet fractions by SDS polyacrylamide gel electrophoresis

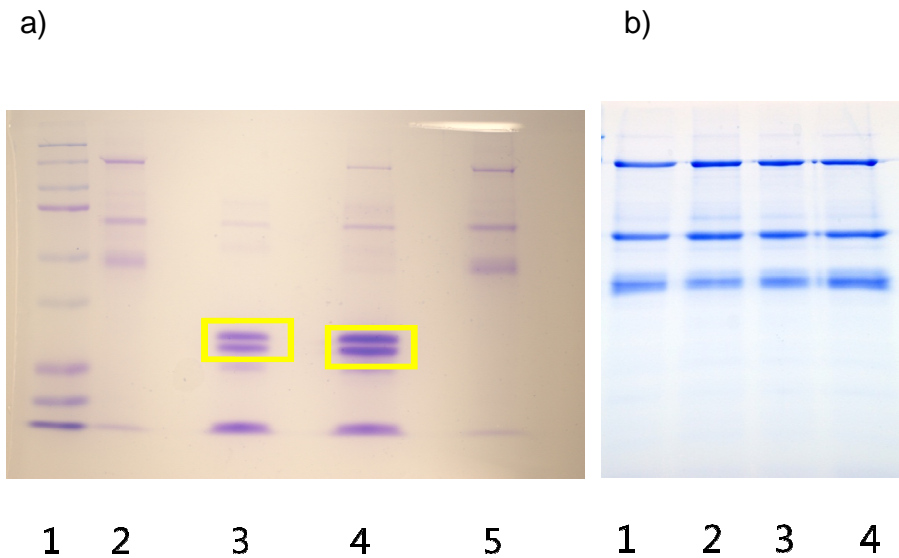
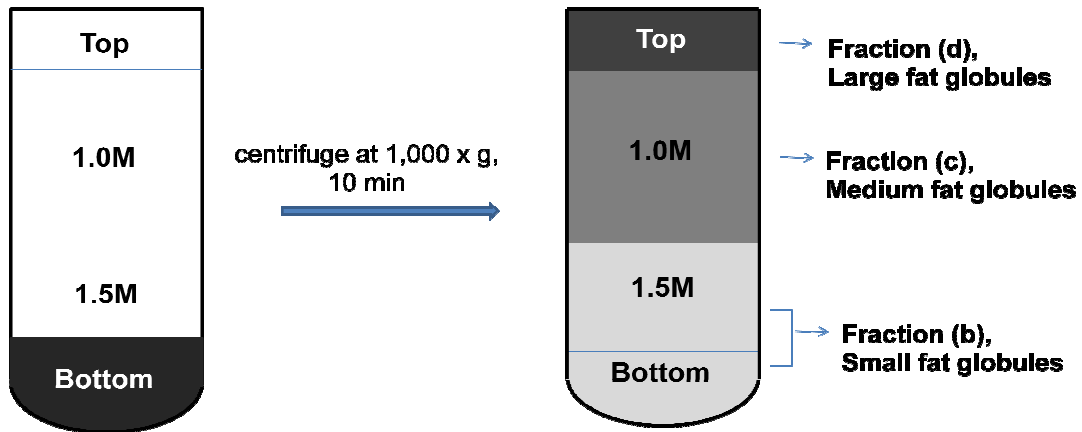


Fig 9. Analysis of lipid droplet protein fractions by SDS-PAGE a) Gel was loaded with equivalent amounts of MFGM according to total protein. Small and medium lipid droplet fractions were contaminated by casein micelles (yellow box). Lane 1, MW standard markers, which were from top to bottom of the gel 250KD, 150KD, 100KD, 75KD, 50KD, 37KD, 25KD, and 20KD; lane 2, whole cream; lane 3, small fraction; lane 4, medium fraction; lane 5, large fraction. b) Modified sucrose gradient fractions following EDTA chelation step, casein micelle contamination was reduced. Lane 1, whole cream; lane 2, small fraction; lane 3, medium fraction; lane 4, large fraction (gel was loaded according to equivalent surface area)

a.



b.

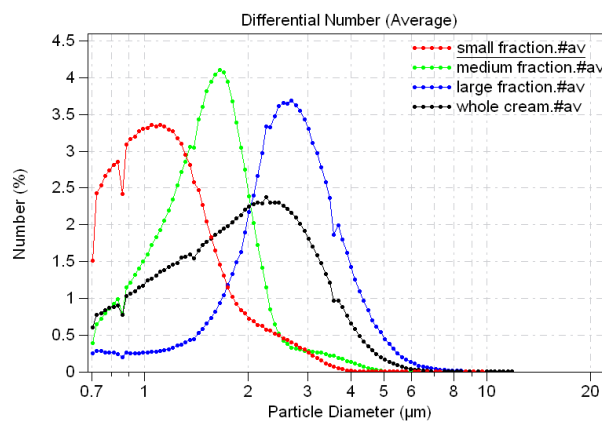


Fig 10. Modified sucrose gradient method a. Whole cream was collected by centrifugation, chelated with EDTA, placed on a sucrose gradient, and centrifuged at 1,000 \times g for 10 min to separate the lipid droplets according to size. b. The size of droplets in each fraction was estimated with a Beckman coulter counter. Average size of lipid droplet in each fraction is $1.26 \pm 0.49 \mu\text{m}$, bottom fraction, (c) $1.58 \pm 0.55 \mu\text{m}$, middle fraction, and (d) $2.72 \pm 0.98 \mu\text{m}$, top fraction.

Bovine cream was collected and fractionated as described above. The mean droplet diameters of fractionated samples were 2.2 μm , for whole cream (unfractionated), 1.26 μm , for the bottom fraction, 1.58 μm , for the middle fraction, and 2.72 μm , for the top fraction (Fig 10b). Fractionated samples and whole cream were stained with Nile red and examined by fluorescence microscopy (Fig 11). Each fractionated sample was analyzed by SDS-PAGE by loading gels based on the same amount of protein, surface area, or neutral lipid (Fig 12). The amount of BTN and XOR was the same regardless of droplet size, whether the gels were loaded according to protein, or surface area. However, as expected, when equivalent amounts of lipid were loaded, the total amount of protein in each lane was higher in the small lipid droplet fractions. This is because the surface area to unit volume ratio is higher in small droplet fractions because they contain more membranes.

Objective 2)

Rationale

According to our working hypothesis, the amount of each MFGM protein that may have a function in secretion or size regulation may have a negative correlation with droplet size. In the first objective, lipid droplets were separated according to their size. To identify absolute amounts of MFGM proteins relative to droplet size, quantitative

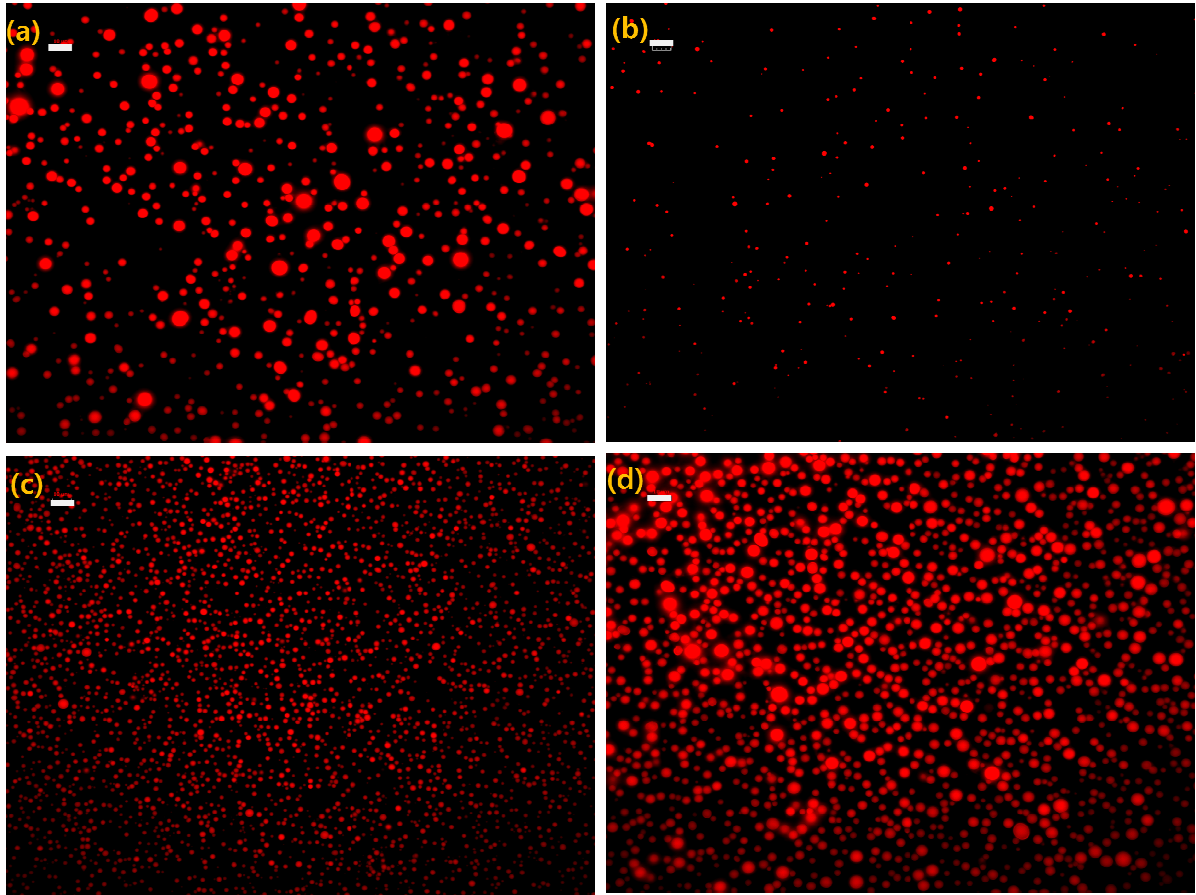


Fig 11. Micrographs of milk-lipid droplet fractions. Droplets were stained with Nile red and examined by fluorescence microscopy. (a) Whole cream, (b) small lipid droplet fraction (bottom), (c) medium lipid droplet fraction (middle), (d) large lipid droplet fraction (top). Bar, 10µm.

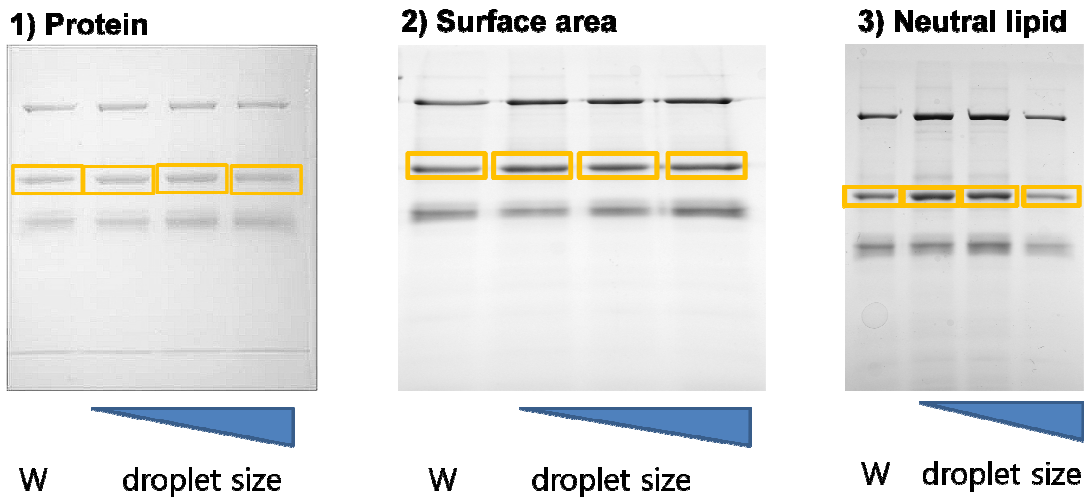


Fig 12. Separation of MFGM proteins in different sized lipid droplets by SDS-PAGE Equivalent amounts of MFGM were loaded according to (1) total protein, (2) total surface area, or (3) neutral lipid. The highlighted rectangular areas indicate BTN in each sample. (1, 2) The amount of BTN in each lipid droplet size is the same if the gels are loaded according to protein, or surface area. (3) However, as expected, samples of larger droplets have proportionally less BTN than smaller droplets when the gels are loaded according to the amount of neutral lipid. W; whole cream, droplet size; small lipid droplet fraction to large lipid droplet fraction from left to right, as indicated.

western blots were performed and the results analyzed by two statistical tests (ANOVA, Tukey's grouping as post hoc, and Principal Component Analysis).

Western blot and quantification

To measure the relative amounts of each specific MFGM protein, samples were separated by SDS-PAGE as above (objective 1), and blotted with specific antibodies to each protein. Protein amounts were related to the protein amount in the unfractionated cream samples to serve as a reference for the relative amounts of proteins in the fractionated samples. The amount of BTN and XOR was not significantly different in the lipid droplet fractions, based on loading according to protein or surface area (Fig 13, 14). However, as with the coomassie-blue stained gels (Fig 12), the small lipid droplet fraction had proportionally more protein than large lipid droplet fractions, based on neutral lipid. Assays for ADPH were complicated by high variability in the intensity of the stained bands on western blots, possibly because of interference from variable amounts of PAS6/7, which migrates with a similar electrophoretic mobility as ADPH in SDS-gels. In comparison of the band intensities in fractionated samples with the controls (whole cream), the amount of ADPH was higher in the small lipid droplet fraction, based on surface area. However, the amount of ADPH, based on protein, was not significantly different according to size (Fig 15). The amount of ADPH, based on neutral lipid, had the same pattern as the amount of other MFGM proteins. i.e., the smaller lipid droplet fractions had more ADPH than larger lipid droplet fractions per unit volume.

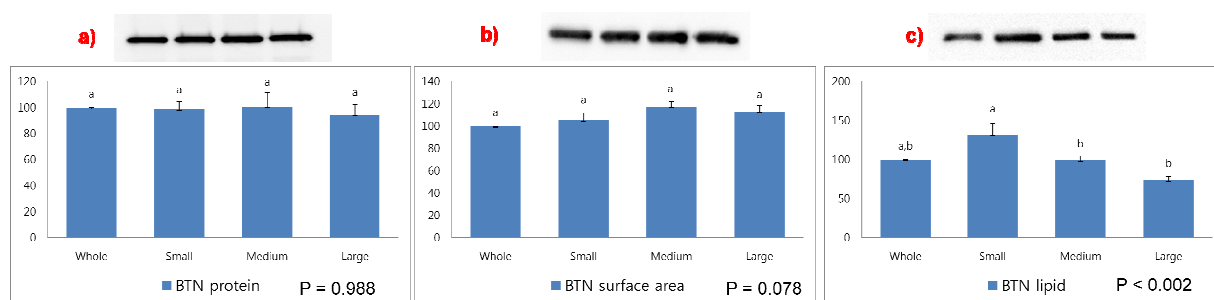


Fig 13. Estimation of the relative amounts of BTN in lipid droplet fractions by quantitative western blot. Five samples were analyzed by western blot with respect to (a) total protein, measured by BCA assay, (b) total surface area, measured with a Beckman multi-sizer (c) total neutral lipid measured by gravimetry. Estimates were normalized to the control sample (whole cream) (100%). There were no significant differences based on protein or surface area, but the amount of BTN was significantly lower (ANOVA) in large droplets based on neutral lipid ($P < 0.002$). Tukey's grouping following ANOVA as statistical test. $N = 5$, Error bar, SEM

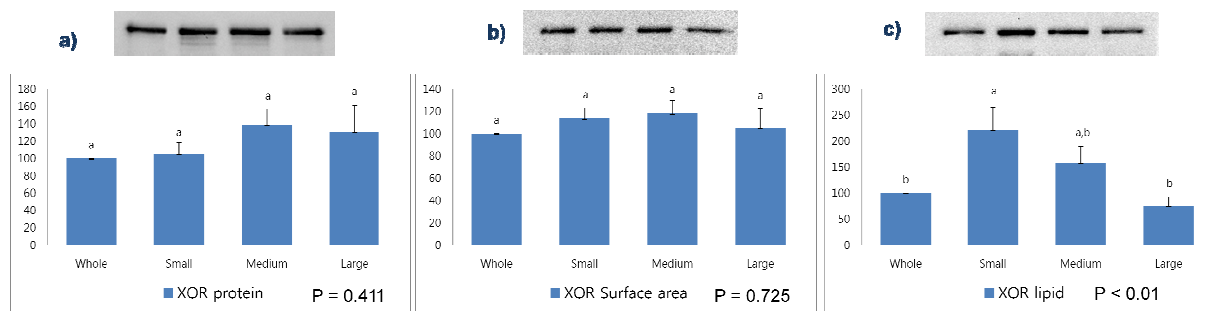


Fig 14. Estimation of the relative amounts of XOR in lipid droplet fractions by quantitative western blot Samples were assayed as described in the legend to Fig 13. There were no significant differences based on protein or surface area, but the amount of XOR was significantly lower in large droplets based on neutral lipid ($P < 0.01$). Tukey's grouping following ANOVA as statistical test. $N = 5$, Error Bar, SEM

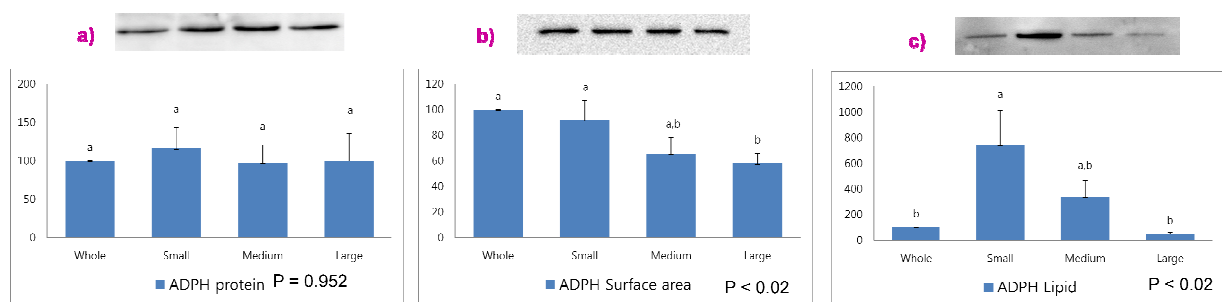


Fig 15. Estimation of the relative amounts of ADPH in lipid droplet fractions by quantitative western blot. Samples were assayed as described in the legend to Fig 13. There were no significant differences based on protein, but the amount of ADPH was significantly lower in large droplets based on surface area ($P < 0.02$) and neutral lipid ($P < 0.02$). Tukey's grouping following ANOVA as statistical test. $N = 5$, Error bar, SEM

In contrast to the other proteins, the amount of CD36 was higher in small lipid droplet fractions, based on both protein ($P < 0.01$) and surface area ($P < 0.0001$) (i.e. 4-fold higher in small lipid droplets than large lipid droplets). CD36 differences on a neutral lipid basis were even more pronounced (Fig 16). Although FABP is a known partner protein of CD36 there was no positive correlation with the amounts of CD36. The amounts of FABP were not significantly different, based on protein or surface area, but they decreased with increasing droplet size on a unit volume basis, similar to the other proteins (Fig 17).

It was impossible to measure the relative amounts of PAS6/7 because there is currently no antibody and the commercial antibody to MFG-E8, which is the homologous mouse protein, does not cross react with bovine PAS6/7.

Principal component analysis (PCA)

PCA was used to assess the inter-relationship between the measured variables. PCA was performed, in order to develop a smaller number of artificial variables (i.e. independent) from the large number of observed variables (i.e. inter-related), which account for most of the variance in the samples. PCA reduces the observed redundancy of variables into a smaller number of principal components. Therefore, PCA is an orthogonal linear transformation that transforms the data into a new coordinate system. Thus, the greatest variance lies on the first coordinate (Component 1), and second

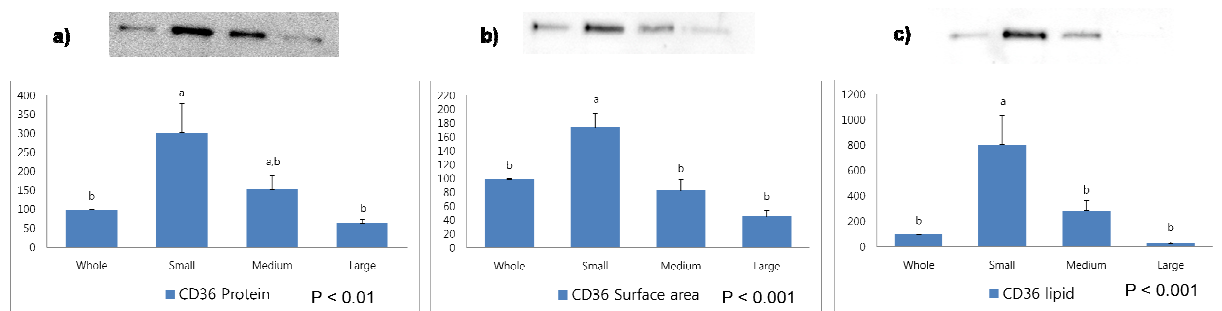


Fig 16. Estimation of the relative amounts of CD36 in lipid droplet fractions by quantitative western blot. Samples were assayed as described in the legend to Fig 13. Small droplets had significantly more CD36 than medium-sized, or large droplets based on protein (P < 0.01), surface area (P < 0.001), or neutral lipid (P < 0.001). Tukey's grouping following ANOVA as statistical test. N = 5, Error bar, SEM

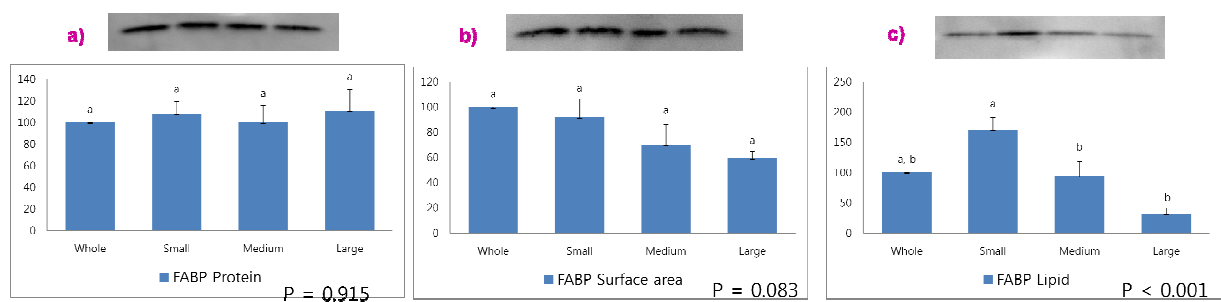


Fig 17. Estimation of the relative amounts of FABP in lipid droplet fractions by quantitative western blot. Samples were assayed as described in the legend to Fig. 13. There were no significant differences based on protein or surface area, but the amount of FABP was significantly lower in large droplets based on neutral lipid ($P < 0.001$). Tukey's grouping following ANOVA as statistical test. $N = 5$, Error bar, SEM

mean diameter, surface area per droplet, lipid volume (%), and the western-blot band intensity of each droplet fraction. FABP intensity was excluded, since the sample number was different from the other proteins. Based upon PCA analysis, the amount of CD36 was negatively correlated with the size of the droplets. In the case of the other proteins, all lipid based band intensities were negatively correlated with surface area and size. However, surface area and protein based western blot intensities of other MFGM proteins were not negatively correlated with size, surface area, and fat (Fig 18). In contrast to the ANOVA test for the amount of ADPH on a surface area basis, the intensity of ADPH in the PCA analysis was not significantly correlated with size.

Correlation coefficients were calculated in order to determine whether these intensities were related to surface area, size, and fat content (Table 1). Based on this analysis, as also observed in Figure 18, all the lipid based MFGM protein intensities had negative correlations with surface area, size, and fat (significantly or a trended to be significant i.e. ADPHI Corr: - 0.45042, P = 0.092 and XORI Corr: - 0.46714, P = 0.079). Considering the small sample size (N = 5), we can accept that all the blot intensities based on lipid were negatively correlated with surface area, size, and fat. For the blot intensities from CD36 westerns loaded on a surface area or protein basis, CD36s was negatively correlated with surface area, size, and fat, and CD36p also tended to be negatively correlated. Most of the other blot intensities based on different loadings of the other MFGM proteins were slightly negatively correlated, but not significantly (significant correlation coefficients are highlighted).

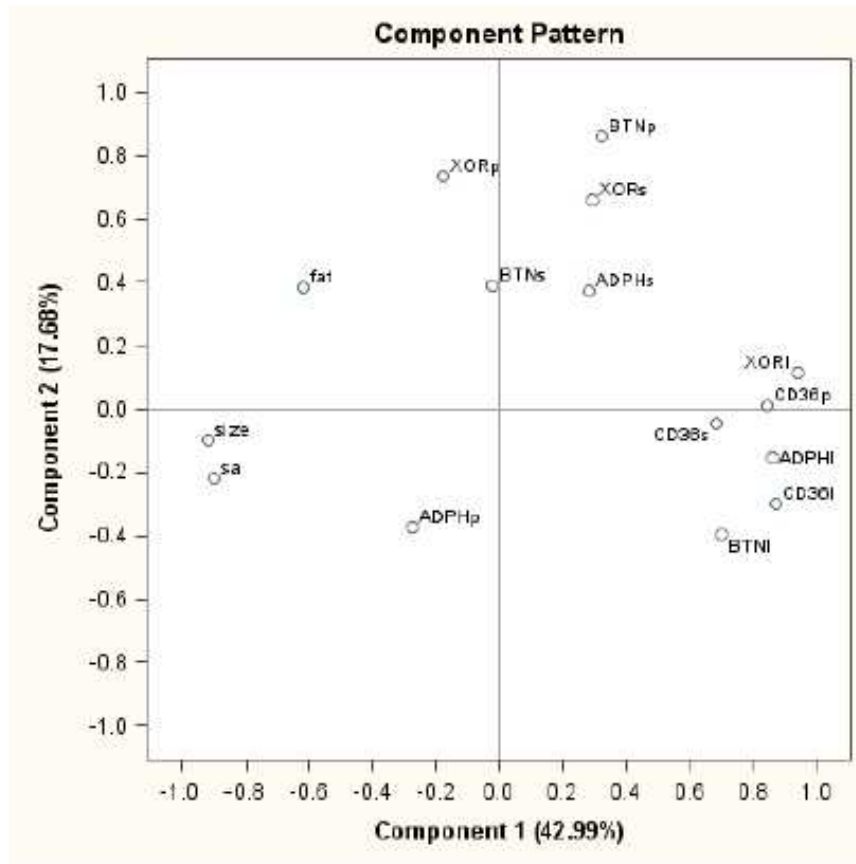


Fig 18. PCA of the amount of protein to the size, surface area, and fat from the western blot data. Loading plot describing the relationship among MFGM proteins by PCA, based on the western blot intensity to the size (μm), surface area (μm^2) and fat volume (%) of the droplets. CD36p (protein loading), and CD36l (lipid loading) are negatively correlated with size, fat and surface area (sa) (The larger size, surface, and lipid, the less CD36 on the droplets). With respect to CD36s (surface area loading), CD36s is negatively correlated with surface area and droplet size and it tends to be significant ($P = 0.07$ to size, $P = 0.10$ to surface area). All the loaded on the basis of lipid protein, including BTN, XOR, and ADPH, are negatively correlated with size and surface area ($P < 0.05$) (the more fat volume, the larger size, then the less protein in the western blots based on neutral lipid).

Table 1. Correlation analysis between western blot intensities and surface area, size, and fat content

The CORR Procedure								
Pearson Correlation Coefficients, N = 15 Prob > r under H0: Rho=0								
	size	sa	fat	ADPHI	BTNI	XORI	CD36I	ADPHs
size	1.00000	0.95913	0.70474	-0.61799	-0.69213	-0.81184	-0.72510	-0.35826
		<.0001	0.0033	0.0141	0.0042	0.0002	0.0022	0.1898
sa	0.95913	1.00000	0.57385	-0.59898	-0.65024	-0.80236	-0.67755	-0.34405
	<.0001		0.0253	0.0183	0.0087	0.0003	0.0055	0.2092
fat	0.70474	0.57385	1.00000	-0.45042	-0.57262	-0.46714	-0.51339	-0.21432
	0.0033	0.0253		0.0920	0.0257	0.0792	0.0503	0.4431
	BTNs	XORs	CD36s	ADPHp	BTNp	XORp	CD36p	
size	-0.05957	-0.25056	-0.47030	0.25699	-0.33733	-0.02727	-0.72900	
	0.8330	0.3677	0.0769	0.3552	0.2189	0.9231	0.0020	
sa	-0.10792	-0.44881	-0.43428	0.28265	-0.41886	-0.02882	-0.72041	
	0.7018	0.0933	0.1058	0.3074	0.1202	0.9188	0.0024	
fat	0.19977	0.17645	-0.24455	-0.17474	0.10152	0.22139	-0.47126	
	0.4753	0.5293	0.3797	0.5334	0.7188	0.4278	0.0762	

In summary, these data indicate that CD36 is more abundant on the surface of small lipid droplets compared with large droplets. In contrast, there were no significant differences in the relative amounts of BTN, XOR, ADPH or FABP on the surface of small, medium and large droplets.

Objective 3)

Rationale

Objectives 1 and 2 were to separate lipid droplets and determine the amount of major MFGM proteins in different sized of lipid droplet fractions by quantitative western blot. There were no differences in the relative amounts of BTN, XOR or FABP, but the amount of CD36 was inversely related to the size of the lipid droplets. The relationship between the amount of ADPH and droplet size was uncertain. In order to confirm these results, we examined the localization pattern and amount of each MFGM protein on the lipid droplets by confocal microscopy. Based on the western blot results, we hypothesized that the amount of CD36 would be higher on the smaller size lipid droplets, and the amount of BTN, XOR, and FABP would be the same regardless of lipid droplet size. ADPH may be negatively correlated with droplet size.

Immunofluorescence microscopy

To determine the distribution of MFGM proteins over the surface of the droplets,

unfractionated samples were stained with specific antibodies to each protein. Scanned images were 3D-reconstructed and fluorescence intensities of the stained droplets were analyzed by Imaris software. Mean fluorescence intensity per droplet was correlated with droplet size. BTN, XOR, ADPH and FABP proteins trended towards higher amounts in the smaller droplets (Figs. 19-22). This trend was most pronounced with CD36, thus confirming the western blot data (compare Fig. 16 with Fig. 23). Most notably, many large droplets were devoid of CD36. The results from the western blot analysis indicated no significant differences in the distribution pattern of MFGM proteins (except for CD36) in different sized of lipid droplets. Considering the fact that the fractionated samples were not entirely small or large, i.e., there were invariably different sized lipid droplets in all the fractions, the decreasing trend observed in fluorescent intensities as droplet size increased is not incompatible with the western blot data.

For comparative purposes, the distribution and amount of specific MFGM proteins as a function of droplet size was also analyzed in mouse lipid droplets by confocal microscopy. Because of the limited amount of mouse milk available, MFGM proteins could not be profiled in different sized lipid droplets employing western blot. Differences in the amount of BTN, ADPH and CD36 on small versus large droplets showed the same trend as with bovine droplets, but the differences were more pronounced (Figs. 24-26). This is probably due to the larger distribution size of mouse milk fat globules (less than 1 to over 10 μm), compared to that of bovine milk fat globules. In addition, MFG-E8 (the mouse homolog of bovine PAS6/7) was also

Fig 19. Analysis of the distribution of BTN on bovine lipid droplets by confocal microscopy. Milk-lipid droplets at peak lactation were fixed in 4% paraformaldehyde. Fixed cream was permeabilized with 0.2% saponin and incubated with specific antibody to bovine BTN followed by goat anti- (rabbit IgG-Alexa 488) as a secondary detecting agent. (a) Bodipy stain for lipid droplets; (b) BTN; (c) merged images, 3D reconstruction; (d) BTN, 2D image. Bars for 3D image, 10 μm ; 2D image, 25 μm . 1) Scatter plot of data obtained with three different animals (color coded); 2) Bar graphs of data from 1) were clustered into five different size categories and Tukey's grouping following ANOVA as statistical test. Mean intensities decreased as droplet size became larger based on the grouping. (N = 1830, P < 0.001, error bar, SEM)

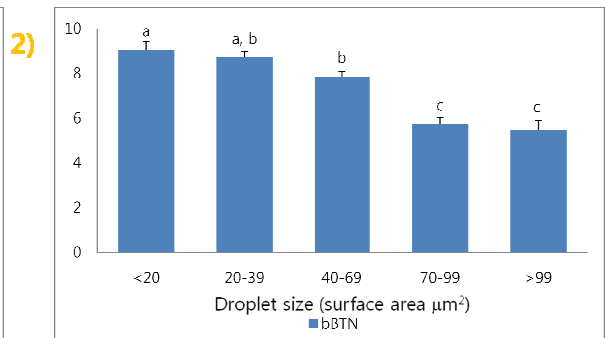
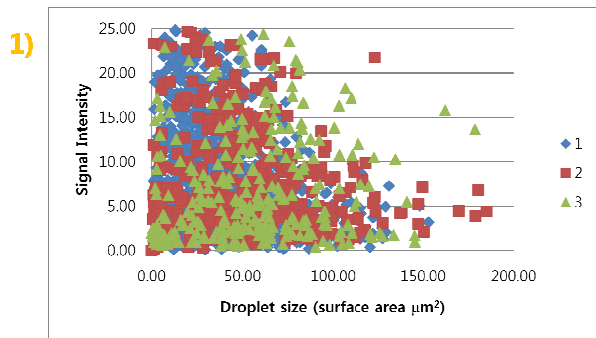
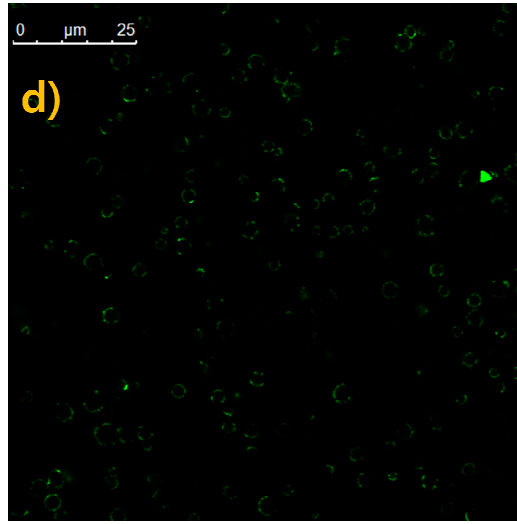
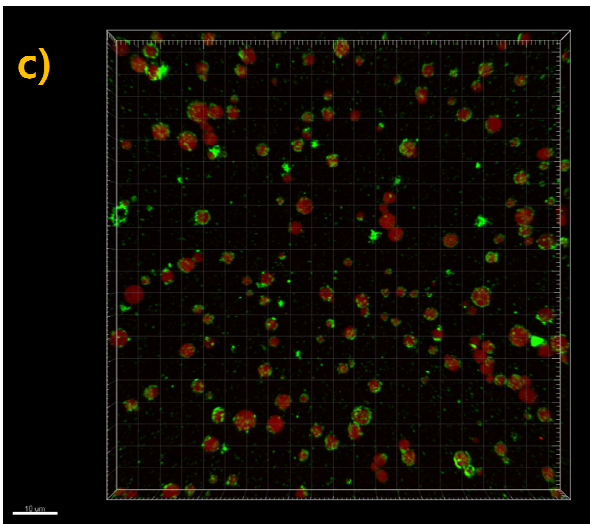
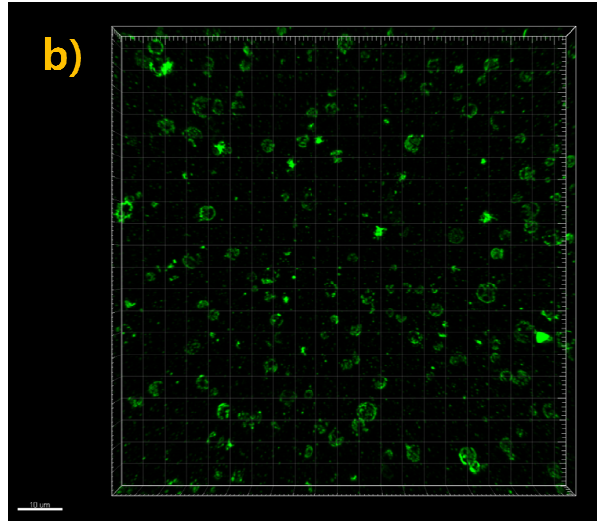
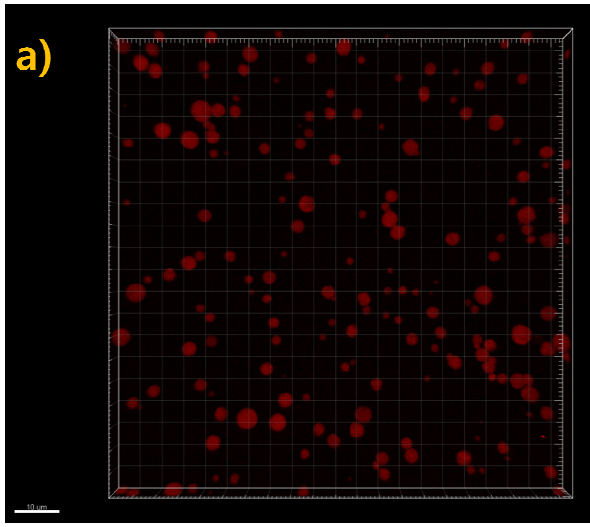


Fig 20. Analysis of the distribution of XOR on bovine lipid droplets by confocal microscopy. Milk-lipid droplets at peak lactation were fixed in 4% paraformaldehyde. Fixed cream was permeabilized with 0.2% saponin and incubated with specific antibody to bovine XOR followed by goat anti- (rabbit IgG-Alexa 488) as a secondary detecting agent. (a) Bodipy stain for lipid droplets; (b) XOR; (c) merged images, 3D reconstruction; (d) XOR, 2D image. Bars for 3D image, 10 μm ; 2D image, 25 μm . 1) Scatter plot of data obtained with three different animals (color coded); 2) Bar graphs of data from 1) were clustered into five different size categories and Tukey's grouping following ANOVA as statistical test. Mean intensities decreased as droplet size became larger based on the grouping. (N = 1989, P < 0.0001, error bar, SEM)

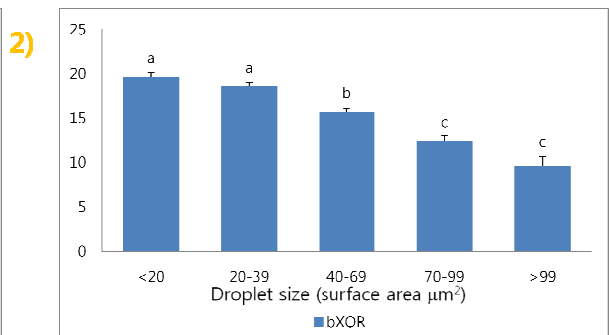
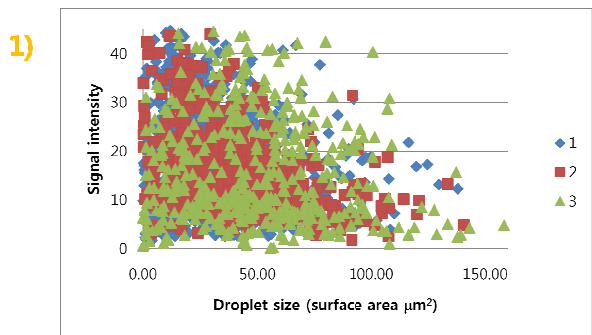
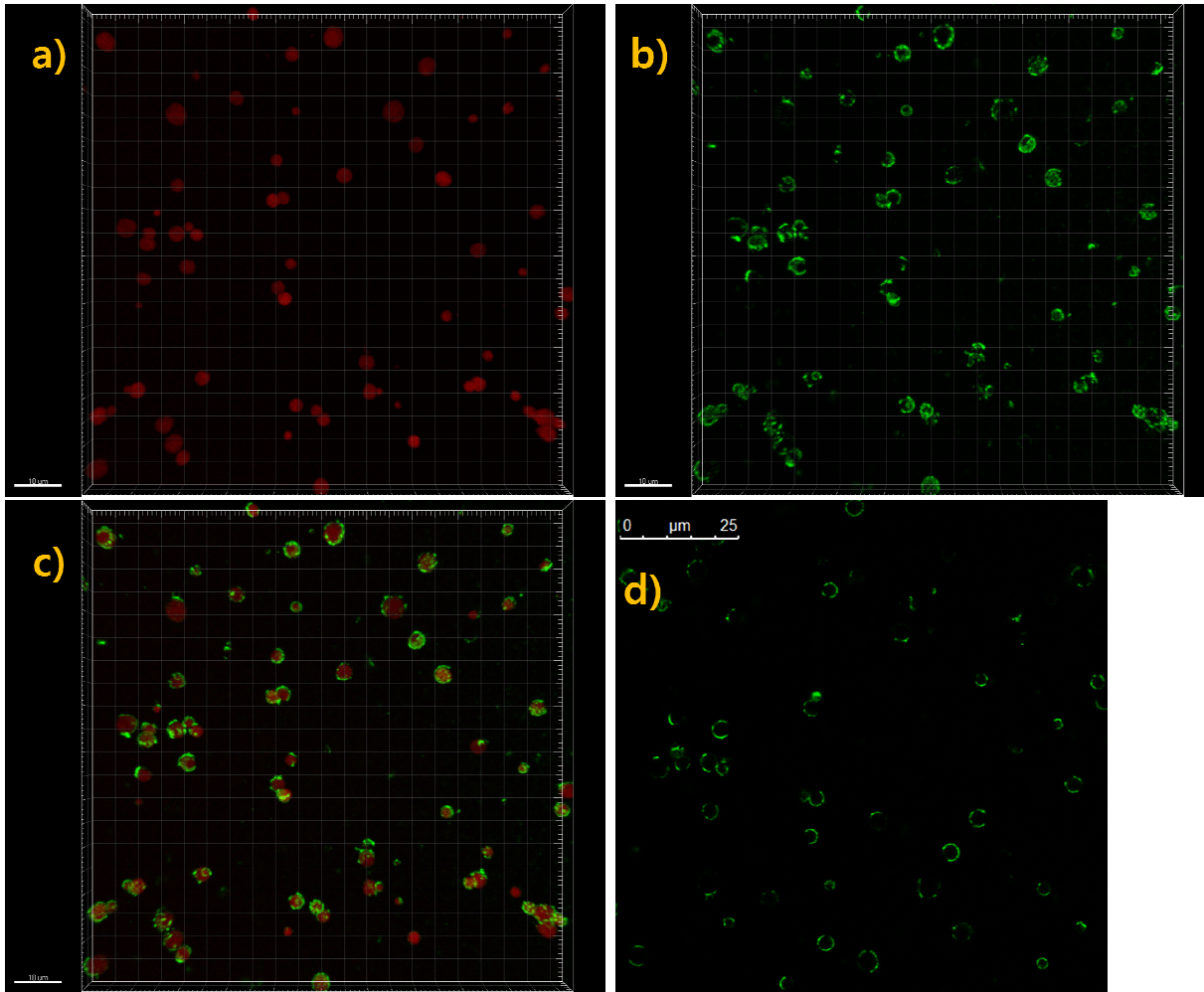


Fig 21. Analysis of the distribution of ADPH on bovine lipid droplets by confocal microscopy. Milk-lipid droplets at peak lactation were fixed in 4% paraformaldehyde. Fixed cream was permeabilized with 0.02% digitonin and incubated with specific antibody to bovine ADPH followed by goat anti- (rabbit IgG-Alexa 488) as a secondary detecting agent. (a) Bodipy stain for lipid droplets; (b) ADPH; (c) merged images, 3D reconstruction; (d) ADPH, 2D image. Bars for 3D image, 10 μm ; 2D image, 25 μm . 1) Scatter plot of data obtained with three different animals (color coded); 2) Bar graphs of data from 1) were clustered into five different size categories and Tukey's grouping following ANOVA as statistical test. Mean intensities decreased as droplet size became larger based on the grouping. (N = 2178, P < 0.0001, error bar, SEM)

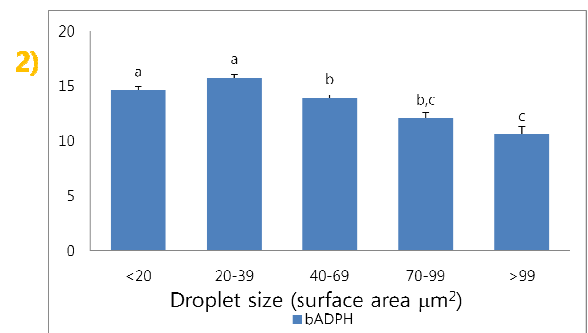
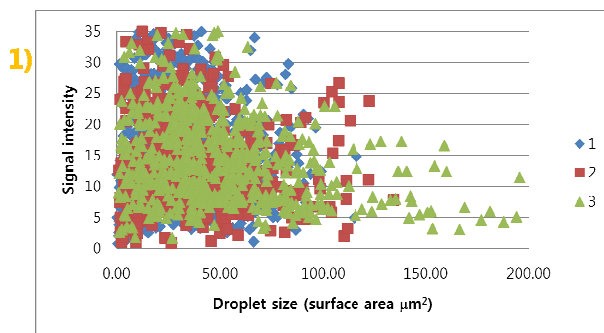
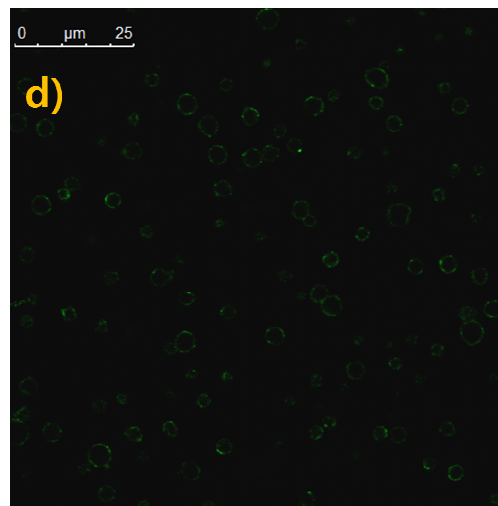
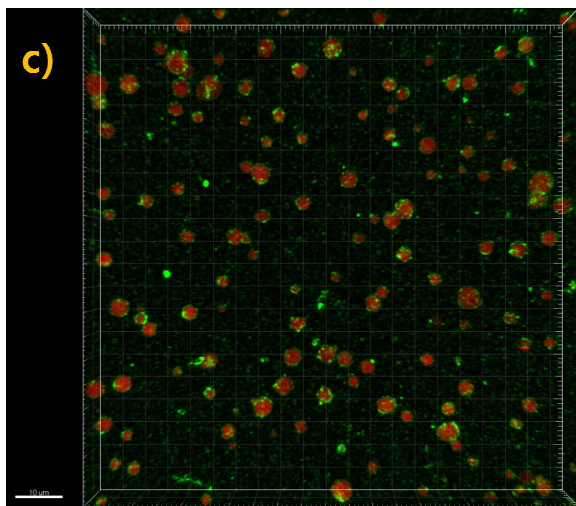
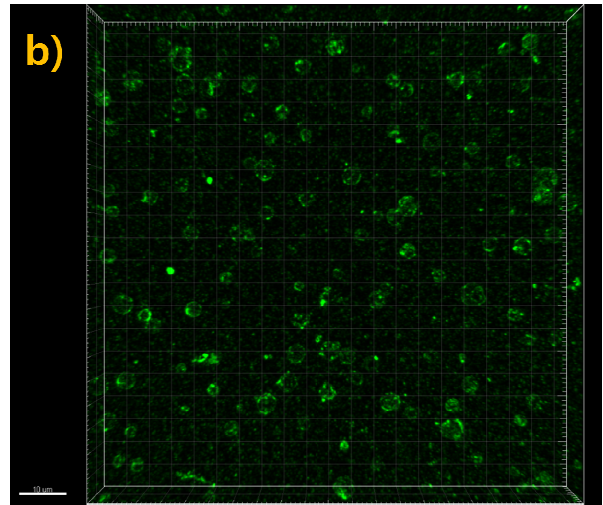
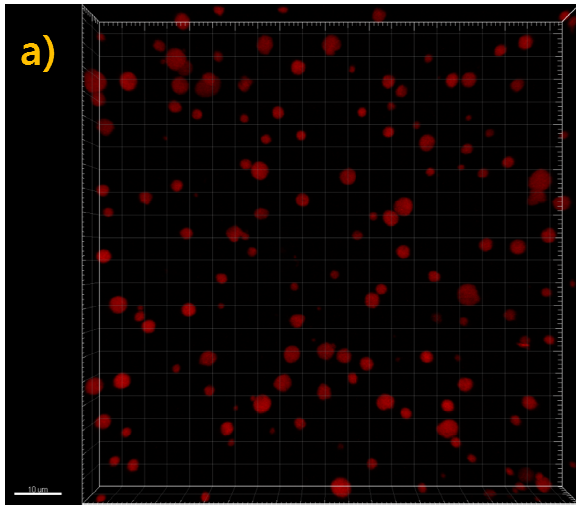


Fig 22. Analysis of the distribution of FABP on bovine lipid droplets by confocal microscopy. Milk-lipid droplets at peak lactation were fixed in 4% paraformaldehyde. Fixed cream was permeabilized with 0.4% saponin and incubated with specific antibody to bovine FABP followed by goat anti- (rabbit IgG-Alexa 488) as a secondary detecting agent. (a) Bodipy stain for lipid droplets; (b) FABP; (c) merged images, 3D reconstruction; (d) FABP, 2D image. Bars for 3D image, 10 μm ; 2D image, 25 μm . 1) Scatter plot of data obtained with three different animals (color coded); 2) Bar graphs of data from 1) were clustered into five different size categories and Tukey's grouping following ANOVA as statistical test. Mean intensities decreased as droplet size became larger based on the grouping. (N = 1655, P < 0.0001, error bar, SEM)

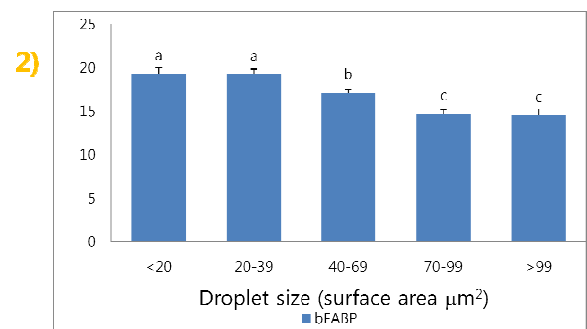
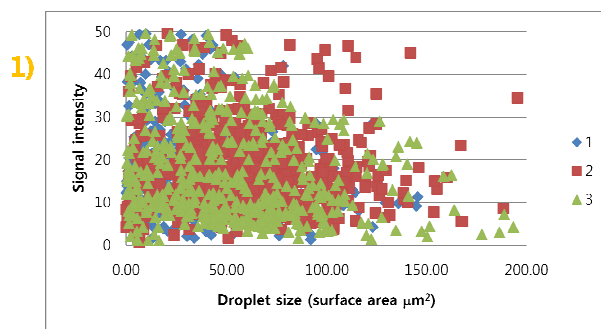
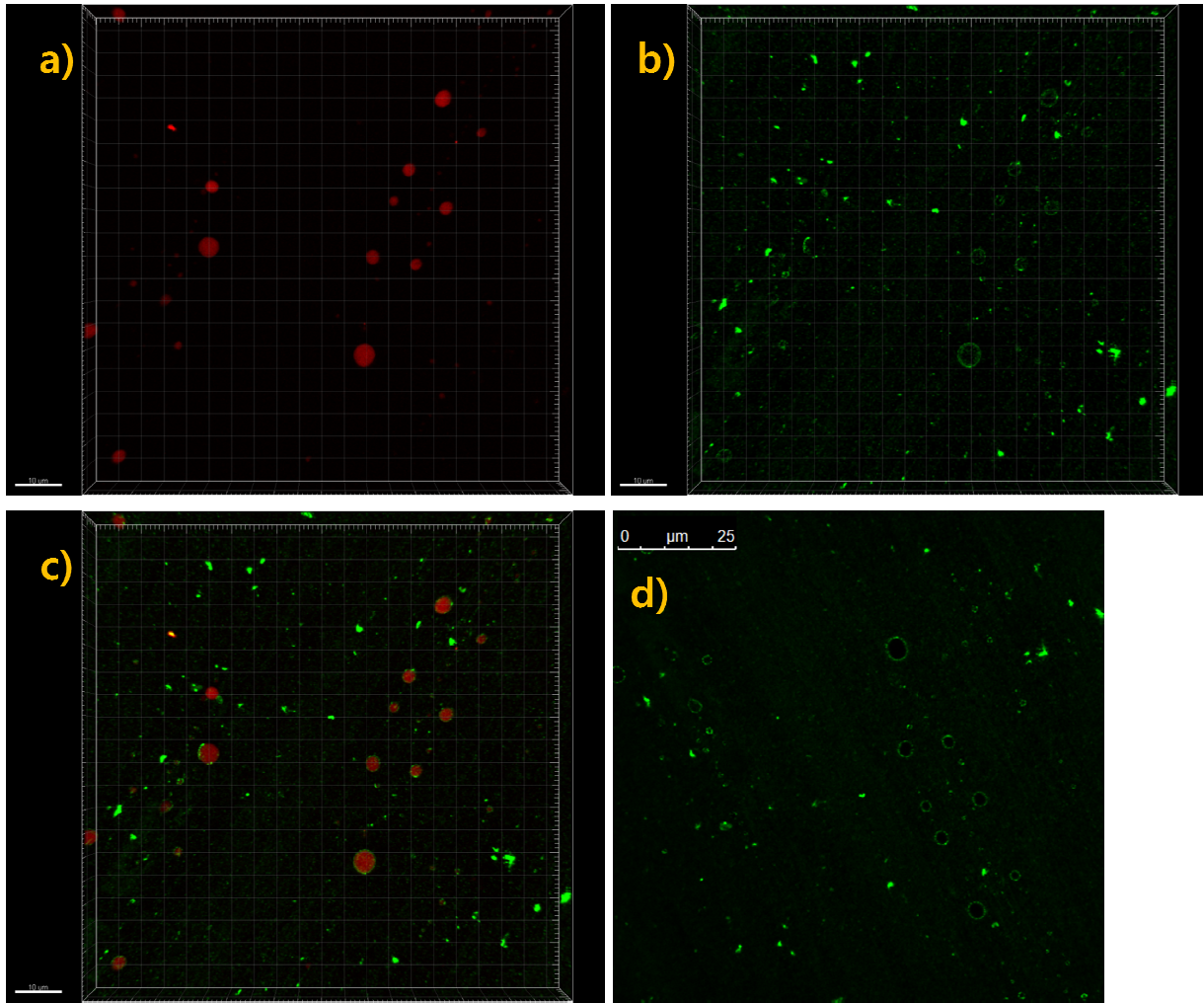


Fig 23. Analysis of the distribution of CD36 on bovine lipid droplets by confocal microscopy. Milk-lipid droplets at peak lactation were fixed in 4% paraformaldehyde. Fixed cream was incubated with specific antibody to human CD36 followed by goat anti-(rabbit IgG-Alexa 488) as a secondary detecting agent. (a) Bodipy stain for lipid droplets; (b) CD36; (c) merged images, 3D reconstruction; (d) CD36, 2D image. Bars for 3D image, 10 μm ; 2D image, 25 μm . 1) Scatter plot of data obtained with three different animals (color coded); 2) Bar graphs of data from 1) were clustered into five different size categories and Tukey's grouping following ANOVA as statistical test. Mean intensities decreased sharply as droplet size became larger based on the grouping. (N = 2319, $P < 0.0001$, error bar, SEM)

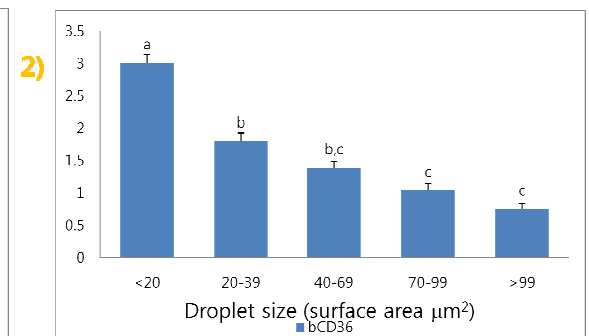
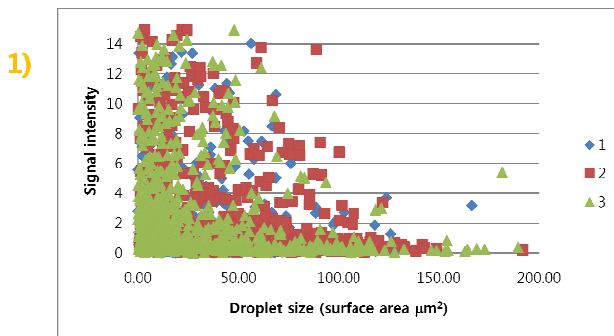
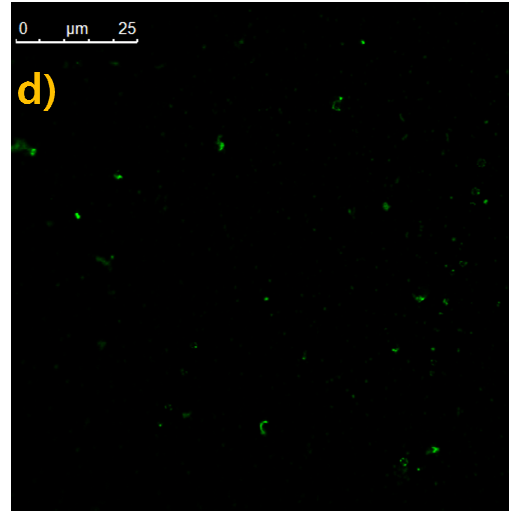
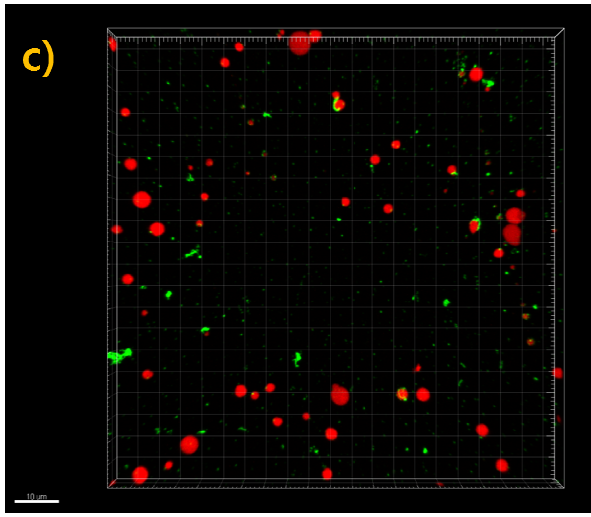
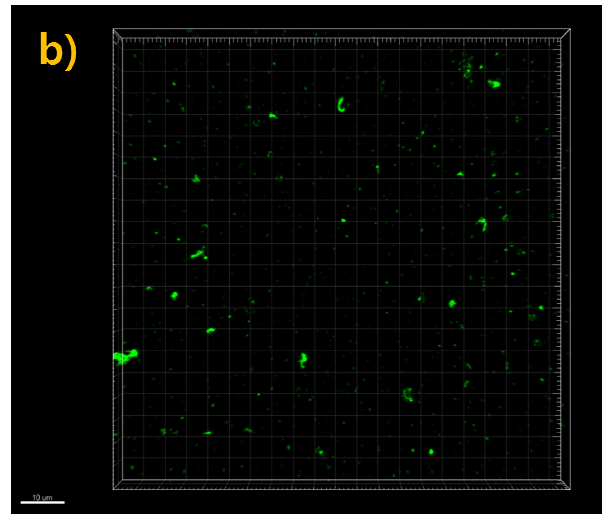
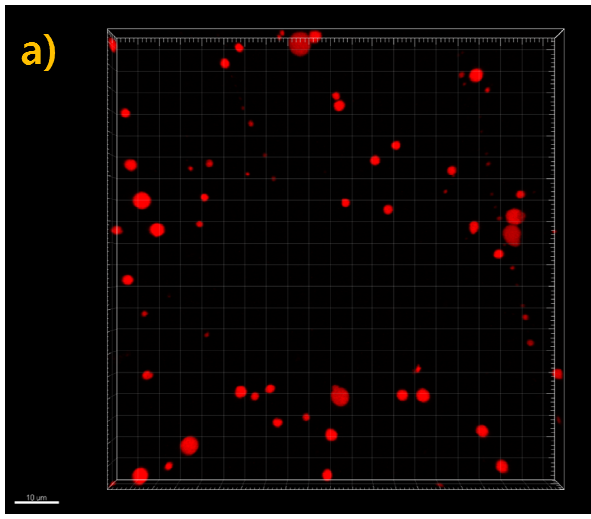


Fig 24. Analysis of the distribution of BTN on mouse lipid droplets by confocal microscopy. Milk-lipid droplets at peak lactation were fixed in 4% paraformaldehyde. Fixed cream was permeabilized with 0.1% Triton X-100 and incubated with specific antibody to mouse BTN followed by goat anti- (rabbit IgG-Alexa 488) as a secondary detecting agent. (a) Bodipy stain for lipid droplets; (b) BTN; (c) merged images, 3D reconstruction; (d) BTN, 2D image. Bars for 3D image, 10 μm ; 2D image, 25 μm . 1) Scatter plot of data obtained with three different animals (color coded); 2) Bar graphs of data from 1) were clustered into six different size categories and Tukey's grouping following ANOVA as statistical test. Mean intensities decreased as droplet size became larger based on the grouping. (N = 609, P < 0.0001, error bar, SEM)

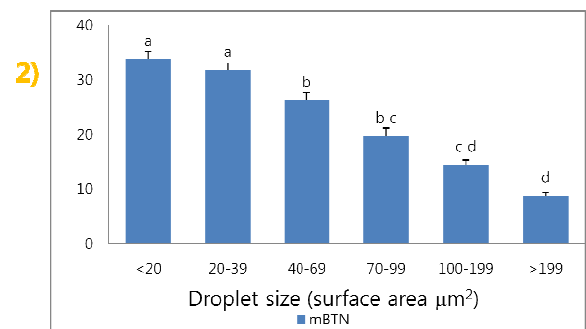
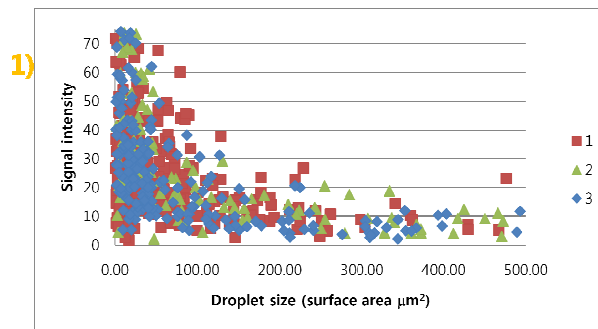
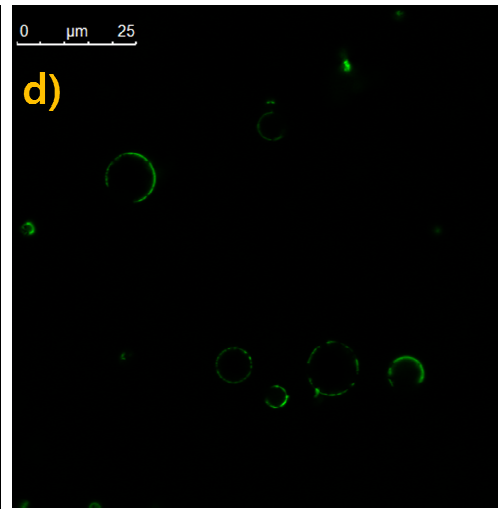
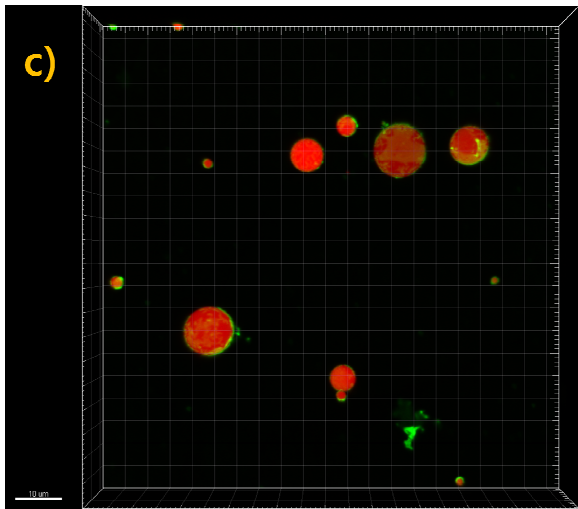
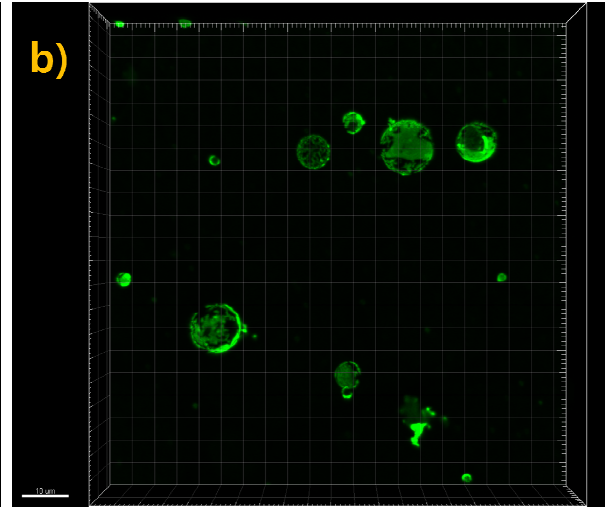
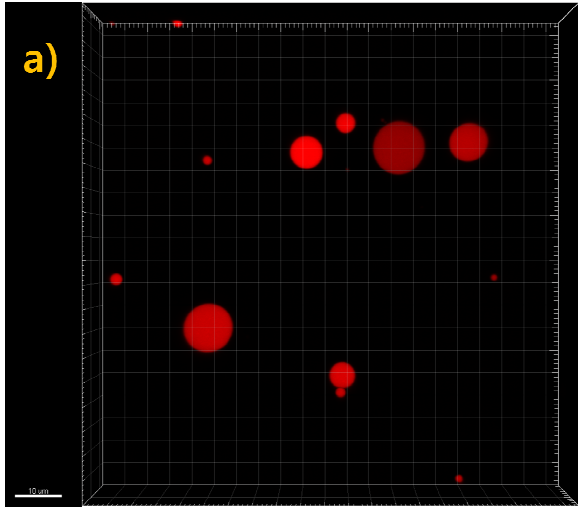


Fig 25. Analysis of the distribution of ADPH on mouse lipid droplets by confocal microscopy. Milk-lipid droplets at peak lactation were fixed in 4% paraformaldehyde. Fixed cream was permeabilized with 0.02% digitonin and incubated with specific antibody to mouse ADPH followed by goat anti- (rabbit IgG-Alexa 488) as a secondary detecting agent. (a) Bodipy stain for lipid droplets; (b) ADPH; (c) merged images, 3D reconstruction; (d) ADPH, 2D image. Bars for 3D image, 10 μm ; 2D image, 25 μm . 1) Scatter plot of data obtained with three different animals (color coded); 2) Bar graphs of data from 1) were clustered into six different size categories and Tukey's grouping following ANOVA as statistical test. Mean intensities decreased as droplet size became larger based on the grouping. (N = 375, P < 0.0001, error bar, SEM)

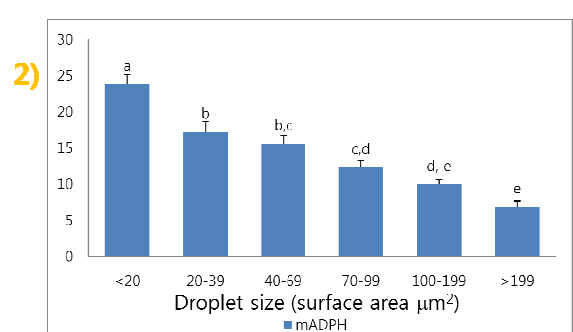
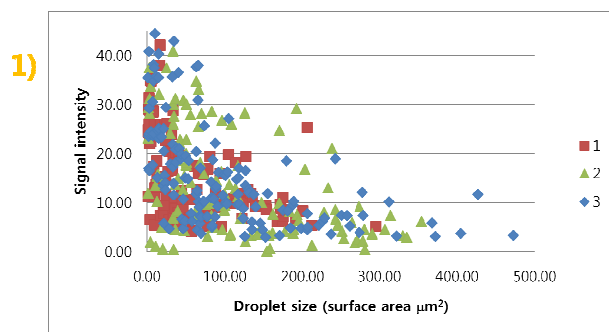
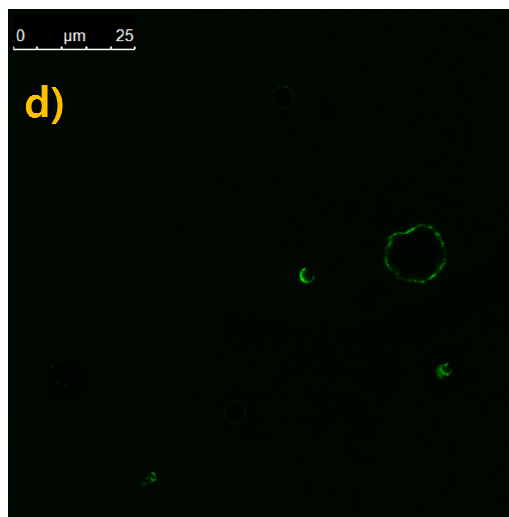
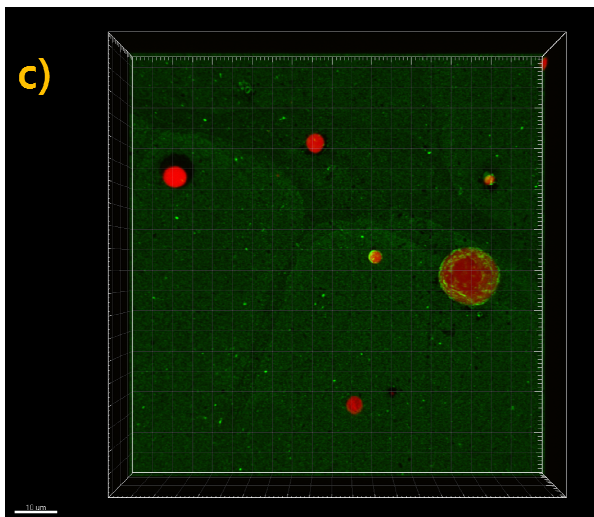
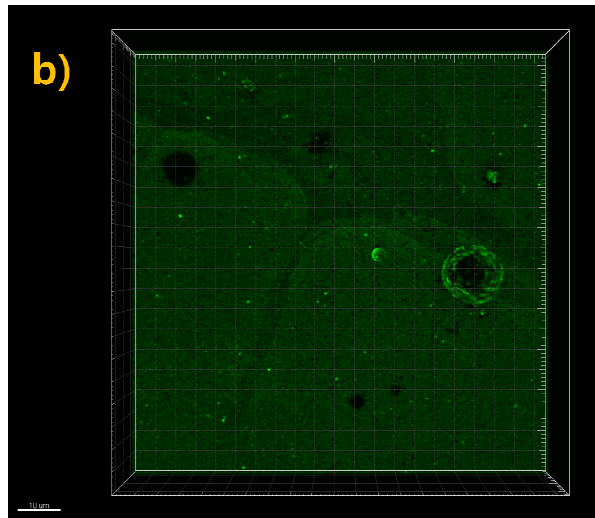
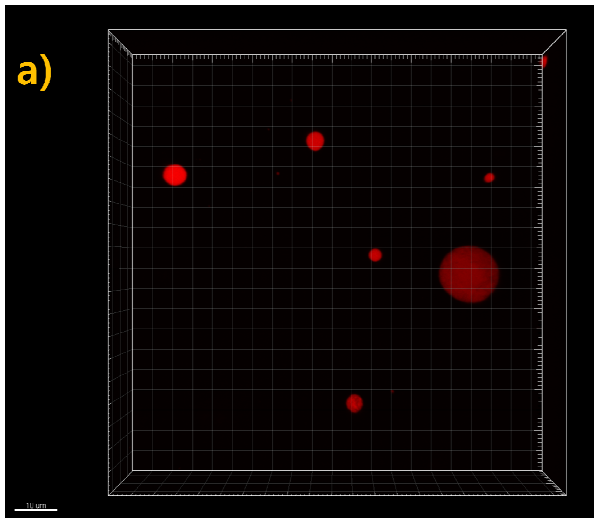
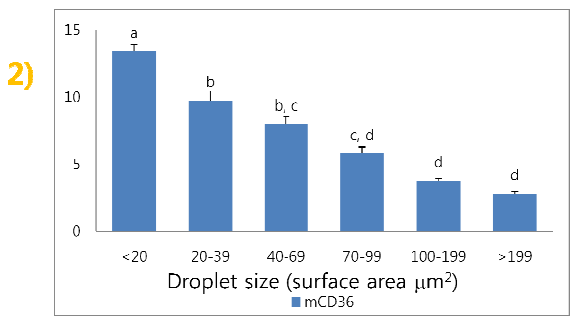
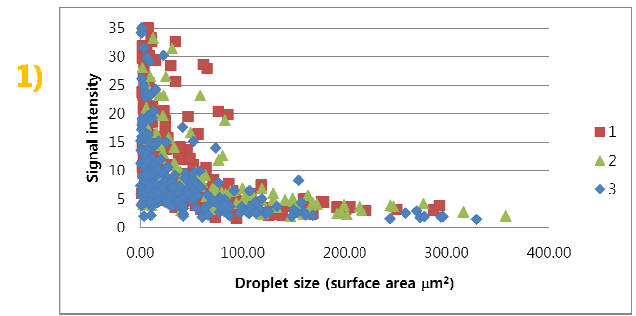
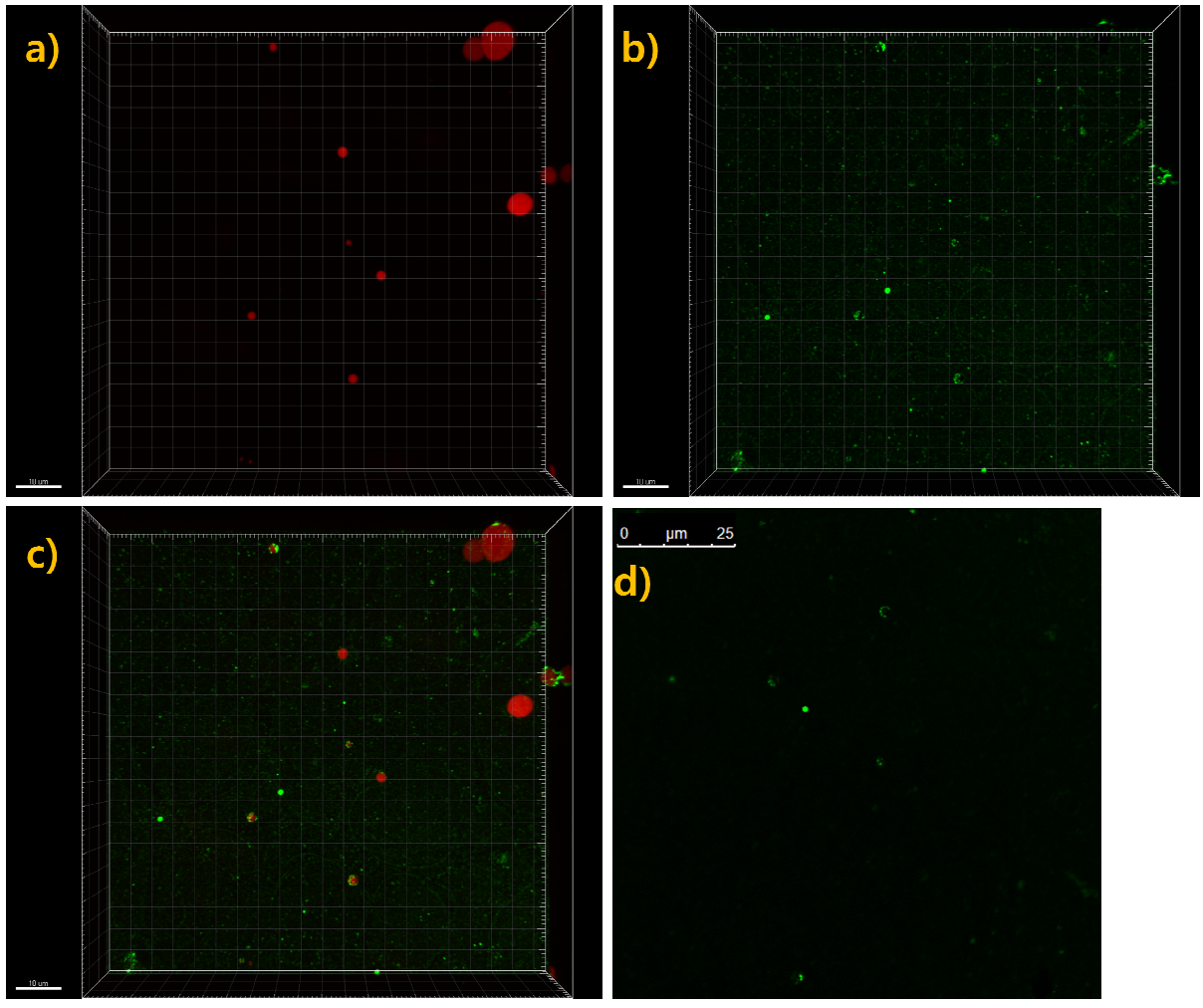


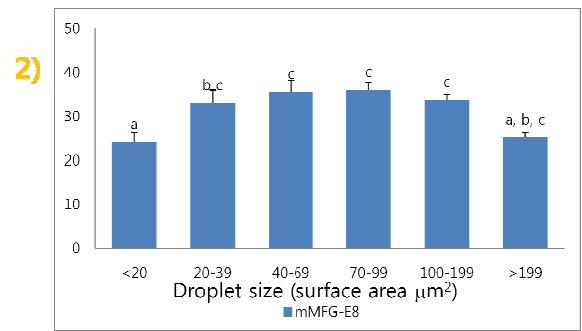
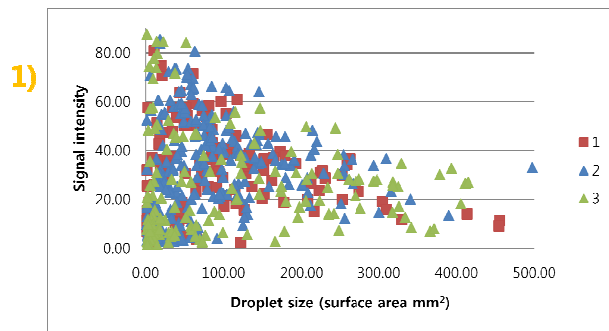
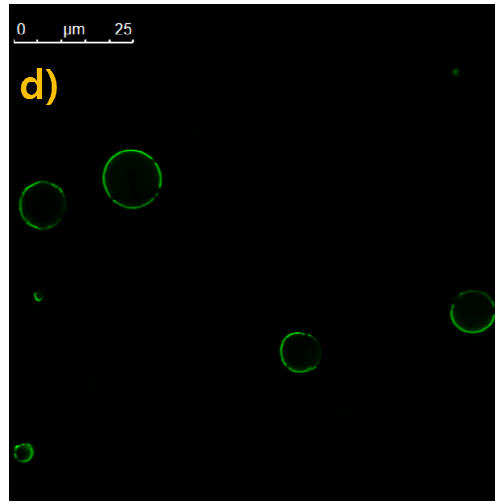
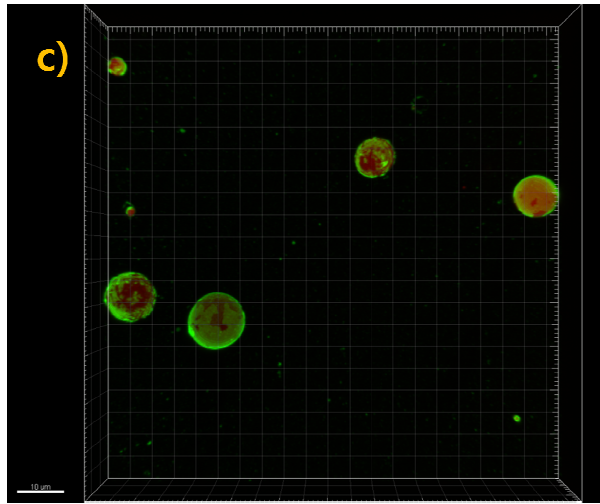
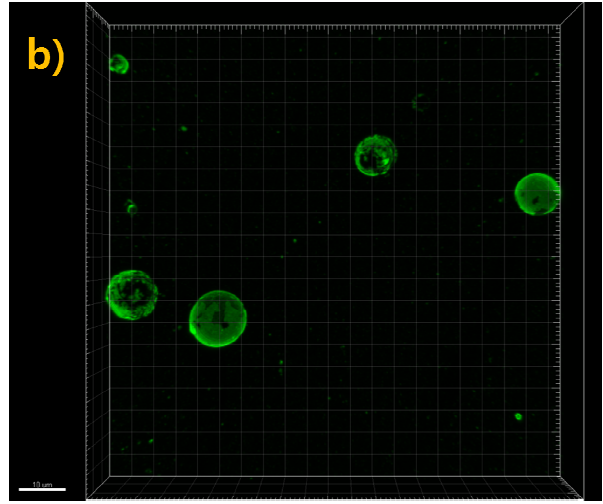
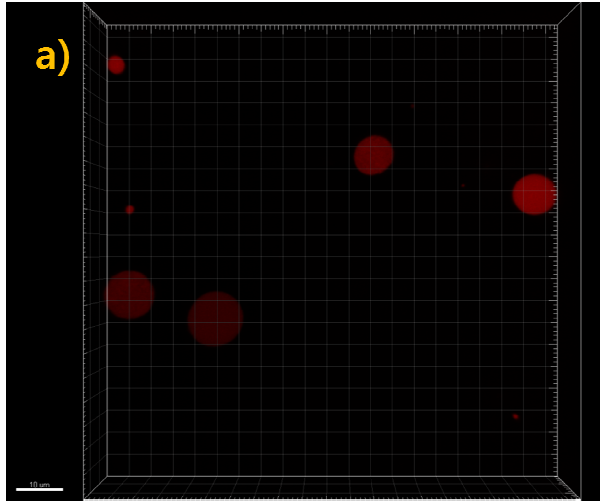
Fig 26. Analysis of the distribution of CD36 on mouse lipid droplets by confocal microscopy. Milk-lipid droplets at peak lactation were fixed in 4% paraformaldehyde. Fixed cream was incubated with specific antibody to human CD36 followed by goat anti-(rabbit IgG-Alexa 488) as a secondary detecting agent. (a) Bodipy stain for lipid droplets; (b) CD36; (c) merged images, 3D reconstruction; (d) CD36, 2D image. Bars for 3D image, 10 μm ; 2D image, 25 μm . 1) Scatter plot of data obtained with three different animals (color coded); 2) Bar graphs of data from 1) were clustered into six different size categories and Tukey's grouping following ANOVA as statistical test. Mean intensities decreased sharply as droplet size became larger based on the grouping. (N = 563, $P < 0.0001$, error bar, SEM)



analyzed, because a commercial antibody was available. In comparison with other MFGM proteins, MFG-E8 was evenly distributed regardless of droplet size (Fig. 27). There was a significant gradual decrease in the amount of BTN and ADPH as the droplet size increased. For both bovine and mouse, CD36 was highly enriched on the small lipid droplets and virtually absent from large lipid droplets.

To confirm that the signal from CD36 was associated with small lipid droplets and not membrane fragments, or exosomes, the small lipid droplet fraction was fractionated into membrane fragments and droplets by ultracentrifugation. The floating layer was presumed to be comprised of small lipid droplets, and the pellet at the bottom of the tube was assumed to consist of membrane fragments or small particles (exosomes?) that may be secreted through other pathways. The fractions were analyzed by western blot (Fig. 28). CD36 was enriched in the floating lipid droplet fraction, confirming that most CD36 is associated with *bona fide* lipid droplets and not membrane fragments. In contrast, BTN was present in both fractions, suggesting that BTN is present on both lipid droplets and unidentified constituents in the membrane fragment fraction.

Fig 27. Analysis of the distribution of MFG-E8 on mouse lipid droplets by confocal microscopy. Milk-lipid droplets at peak lactation were fixed in 4% paraformaldehyde. Fixed cream was incubated with specific antibody to mouse MFG-E8 followed by goat anti- (rabbit IgG-Alexa 546) as a secondary detecting agent. (a) Bodipy stain for lipid droplets; (b) MFG-E8; (c) merged images, 3D reconstruction; (d) MFG-E8, 2D image. Bars for 3D image, 10 μm ; 2D image, 25 μm . 1) Scatter plot of data obtained with three different animals (color coded); 2) Bar graphs of data from 1) were clustered into six different size categories and Tukey's grouping following ANOVA as statistical test. Mean intensities decreased as droplet size became larger based on the grouping. (N = 514, P < 0.0001, error bar, SEM)



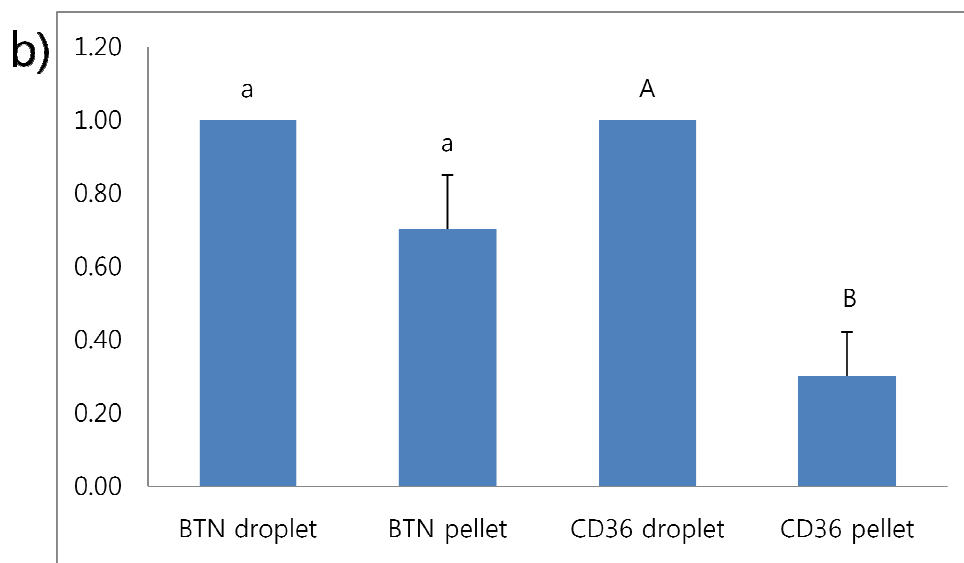
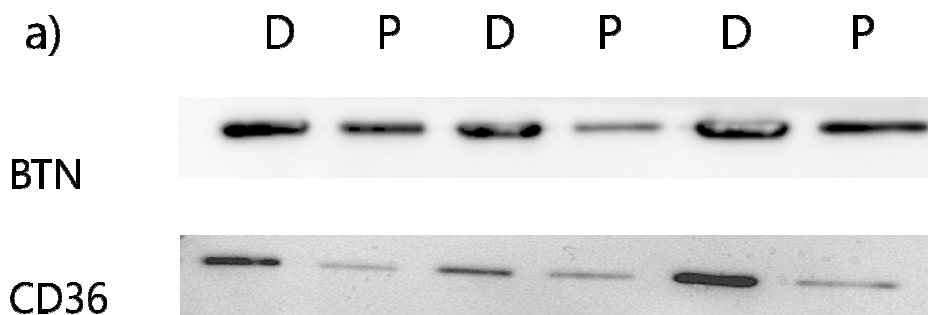


Fig 28. Comparison of the amount of BTN and CD36 in small droplet and pellet fractions. The small lipid droplet fraction was separated by ultracentrifugation into floating (small lipid droplet) and pellet (membrane) fractions. a) proteins were compared by western blot in droplet and pellet. Data from 3 animals. b) the intensity of each band was analyzed by densitometry. The amount of BTN in the droplet fractions and pellets are not significantly different ($P = 0.112$). In contrast, the amount of CD36 was higher in the droplet fraction compared with the pellet fraction ($P < 0.01$). D, droplet; P, pellet; Statistical test, ANOVA and Tukey's grouping test; Error bar, SEM

Discussion

Studies using knock-out mice of either BTN or XOR genes show severe disruption in milk lipid secretion which is associated with increases in lipid droplet size [45, 48]. Furthermore, BTN and XOR interact by binding to each another through the B30.2 domain in the cytoplasmic domain of BTN [36]. Therefore, we hypothesized that interaction between MFGM proteins may serve an important role in the regulation of droplet size. To gain some insight into this possibility, the distribution of BTN, XOR and other MFGM proteins was compared on droplets of different sizes from both bovine and mouse milk. Major findings from this study are discussed separately below: -

1) Practical methods were devised for separating lipid droplets according to their size in Objective 1. Most well-established separation methods are based on separation by unit gravity [62] or sucrose gradient centrifugation [64]. A new method was developed, whereby milk lipid droplets were fractionated from contaminating casein micelles via a modified sucrose gradient method and treatment of the cream samples with 1mM EDTA. Employing this method, lipid droplets were fractionated into small (0.7 - 1.3 μm), medium (1.3 - 1.8 μm), and large (2.0 - 4.0 μm) droplet sizes. Droplet size was measured with a Beckman multisizer, which is adequate for droplets larger than 0.7 μm and smaller than 10 μm in diameter. However, the known minimal size of bovine milk-lipid droplets is 0.2 μm [65]. Therefore, in future studies, fluorescence activated particle sorting (FAPS) by flow cytometry could be used to obtain more accurate distribution

profiles for each fraction [66]. Employing this method, particle profiles could be analyzed with diameters as low as 100nm in diameter and accurate estimates obtained for many of the exceptionally small lipid droplets that are mixed in each fraction.

2) Differences in the distribution of MFGM proteins among fractionated lipid droplets, estimated by quantitative western blot, were identified in Objective 2. Contrary our working hypothesis, the amounts of BTN and XOR were not significantly different in the three fractions (Figs. 13, 14). FABP also appeared to be evenly distributed among small, medium, and large lipid droplets (Fig. 17). The amount of ADPH was higher in the small lipid droplet fraction when samples were loaded according to surface area for the western blots. However, it is not clear whether there was a true difference in the different fractions because of possible interference with PAS 6/7, proteins with similar molecular weights which co-migrate with ADPH during electrophoresis. PCA and correlation analysis in all studied MFGM proteins except for ADPH were consistent with the western blot data. ADPH was not significantly correlated with size, surface area, and fat. However, this approach can only distinguish major differences in protein amounts between the three sizes of fractions, because separation of the lipid droplets was incomplete and even the large lipid droplet fraction was contaminated with very small droplets.

The protein that differed markedly in concentration was CD36, which was concentrated on many of the small lipid droplets and was virtually absent from the large droplets ($>2.75\mu\text{m}$) (Fig. 16). This result was unexpected and novel. To confirm the

CD36 data and to search for more subtle differences in protein amounts between the fractions, confocal microscopy was employed under Objective 3. By imaging the milk lipid droplets, differences in protein amounts on each droplet could be assessed directly, thus overcoming the limitations of analyzing partially fractionated droplet fractions.

3) In Objective 3, the protein distribution and amounts of several MFGM proteins were determined on droplets of different sizes. In addition, for comparative purposes, milk samples from two different species, dairy cow and mouse, were analyzed. The average size of mouse lipid droplets ($6.21 \pm 0.24 \mu\text{m}$) was larger than the cow ($2.97 \pm 0.26 \mu\text{m}$), and therefore there was the potential for interesting differences in protein distributions [67]. Estimation of the amount of MFGM protein from fractionated milk lipid globules using western blot was not possible with mouse milk samples because of the small amount of milk available from each mouse at any given time point.

In contrast to the western blot data, BTN, XOR, ADPH and FABP levels gradually decreased in amount from small sized lipid droplets to large droplets in both species (Figs. 19-22, 24-25, 27). These confocal data are presumably a more accurate reflection of the *in situ* protein distribution because the relative amount of each protein can be determined on each droplet. In agreement with the western blot data, CD36 was concentrated on the small droplets in both dairy cow and mouse, and virtually absent from the large droplets.

Most of the proteins analyzed (BTN, XOR, CD36, ADPH and FABP) were unevenly distributed around the droplet surface, an observation in agreement with

previous studies showing that glycoproteins and glycolipids (identified with lectins) are clustered in patches and rafts [68-70]. These results imply that the MFGM undergoes structural rearrangement after secretion, and that some proteins become clustered in the plane of the bilayer, in agreement with electron microscope data, which showed thickening of protein coat structures on the secreted droplets [54].

Another finding from Objective 3 was the importance of proper fixation and permeabilization procedures for each MFGM protein. Different detergents were used for each protein as explained in the previous section. Depending on the location of proteins and epitopes, either on the exoplasmic side of the bilayer or between the bilayer and lipid droplet surface, different detergents were required for antibody access without impairing the membrane structure. One limitation of confocal microscopy is that droplets less than 1 μm in diameter are difficult to resolve. This limitation could be overcome by using super-resolution fluorescence microscopy [71].

In summary, the data show that XOR, BTN, ADPH and FABP are more highly concentrated on smaller droplets and that CD36 is almost exclusively localized on small droplets. All of these proteins are unevenly distributed over the surface of the droplets in patches. In contrast, the amount of MFG-E8/ μm^2 appears to be about the same regardless of droplet size and the protein covers most of the droplet surface.

These results, in combination with the known topologies of each protein and their potential binding partners, suggest a revised model for the structure of the MFGM and the potential role of MFGM proteins in lipid secretion (Fig 29). The results suggest that

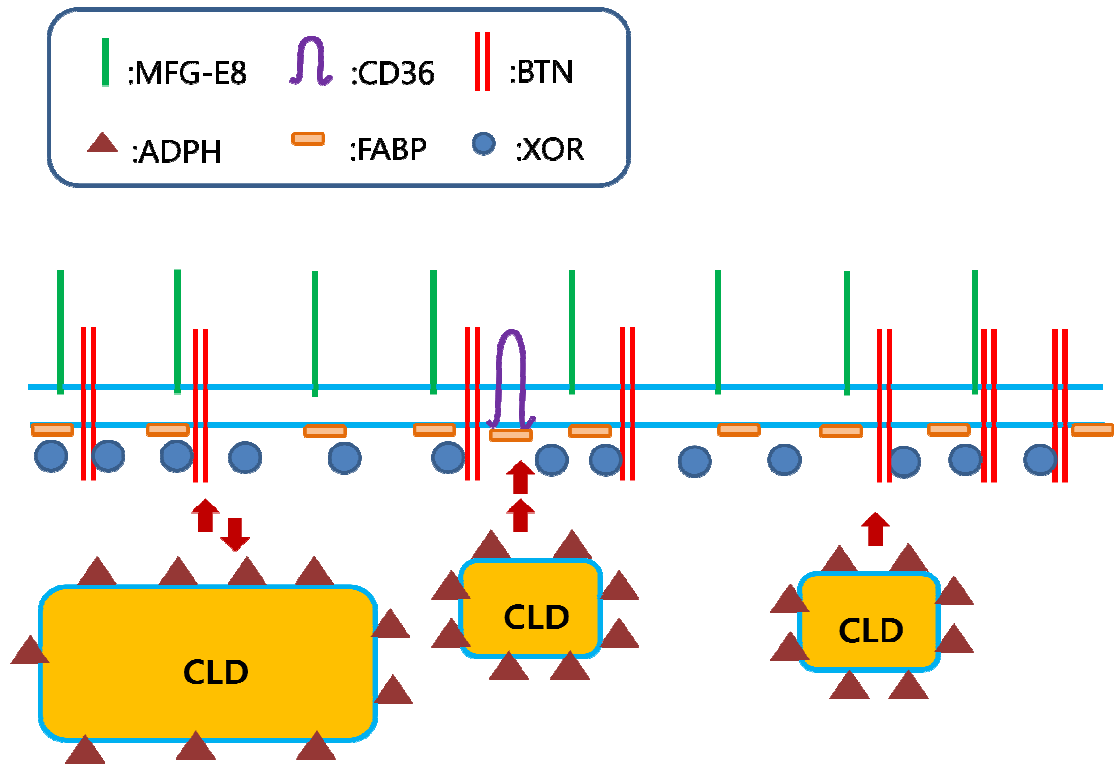


Fig 29. Potential topology of MFGM proteins at the apical surface of mammary epithelial cells. A model was constructed based on previous data [36] and protein distributions discussed in this thesis. XOR and FABP are localized in the cytoplasm. BTN is localized as a transmembrane protein with a lateral heterogeneous pattern. ADPH is localized on the phospholipid monolayer of the lipid core. MFG-E8 is evenly distributed on the epithelial cell membrane. Once CD36 interacts with FABP, small sized cytoplasmic lipid droplets are secreted rapidly (center droplet), some small lipid droplets without CD36 are also secreted, or if not, CLD secretion is delayed and droplets accumulate. Unidirectional arrows indicate a rapid secretion via CD36 and FABP interactions, single arrow indicates BTN / XOR / ADPH mediated secretion without CD36 with small lipid droplets (right hand droplet) and bidirectional arrows indicate a delayed secretion of large lipid droplets (left hand droplet)

some proteins, such as BTN and XOR, are aggregated together in clusters in the place of the lipid bilayer possibly in a binding condition-dependent manner. In contrast, MGF-E8 (mouse PAS 6/7), is uniformly distributed in the outer leaflet of the bilayer by interaction through the C-terminal amphipathic helix [36].

The working hypothesis of this study was that more interactions lead to the rapid secretion of lipid droplets from epithelial cells according to the previous gene disruption studies [45, 48]. As discussed in the Introduction, there are three models that have been proposed to explain how lipid droplets are secreted. In the first model, Mather and Keenan suggested that interaction between BTN and XOR is required for the formation of the outer envelope of MFGM and the expulsion of droplets [29]. However, the results from this study suggest that other MFGM protein interactions also may be required for the secretion of small lipid droplets. Two well-known binding partners among the major MFGM proteins are BTN to XOR and CD36 to FABP. Binding of BTN to XOR was characterized by *in vitro* assays. Interaction is through the B30.2 domain of BTN at neutral pH, which may be necessary for secretion [37]. Additionally, the interaction between CD36 and FABP by immunoprecipitation experiments was revealed [38]. Contrary to other MFGM proteins, CD36 was concentrated on smaller droplets, while it was almost absent on larger droplets according to both western blot and immunofluorescence data (Fig. 16, 23, 26).

Based on these results, a dynamic model of lipid secretion is postulated – if small droplets bind to sufficient protein aided by CD36 and FABP, they will be secreted rapidly.

If insufficient protein is available, the droplets increase in size at the plasma membrane and BTN-XOR interactions become more important before droplets are secreted. This hypothesis is consistent with the observations that there is more protein on smaller droplets, and CD36 is exclusively concentrated on the small droplets.

The functions of CD36 in fatty transport and lipid metabolism have been clarified, but no function associated with milk lipid droplet secretion from CD36-null mice has been clearly identified [72]. In order to confirm the suggested function of CD36, CD36 or FABP tissue-specific knock-out mouse strains could be analyzed or the effect of knock-down or over-expression of these genes assessed in transgenic mouse lines. If the interaction between CD36 and FABP is impaired in knock-out or 'knock-down' mouse lines, the milk should contain fewer small lipid droplets. On the other hand, over-expression of CD36 should induce an increased secretion of small droplets, with a concomitant decrease in the larger droplets typical of mouse milk.

References

1. Neville, M. C. Lactogenesis in women: A cascade of events revealed by milk composition. In *The Composition of Milks*, ed. Jensen, R. D. 1995b: pp. 87-98. San Diego: Academic Press.
2. Turner, M.D., Rennison, M. E., Handel, S. E., Welde, C. J. & Burgoyne, R. D. *Proteins are secreted by both constitutive and regulated secretory pathways in lactating mouse mammary epithelial cells*. *J.Cell Biol.*, 1992. **117**: p. 269-278.
3. Lin, Y., Xia, L., Turner, J. D. & Zhao, X. *Morphologic observation of neutrophil diapedesis across bovine mammary gland epithelium in vitro*. *American Journal of Veterinary Research*, 1995. **56**: p. 203-207.
4. Neville, M.C. and Picciano, M.F. *Regulation of milk lipid secretion and composition*. *Annu. Rev. Nutr.*, 1997. **17**: p. 159-184.
5. Cavaletto, M., Giuffrida, M.G. and Conti, A. *Milk fat globule membrane components - A proteomic approach*, in *Bioactive Components of Milk*. 2008. p. 129-141.
6. Mather, I.H. and Keenan, T.W. *Origin and secretion of milk lipids*. *J. Mammary Gland Biol. Neoplasia*, 1998. **3**: p. 259-273.
7. Hansen, H.Q., Grunnet, I., and Knudsen, J. *Triacylglycerol synthesis in goat mammary gland. Factors influencing the esterification of fatty acids synthesized de novo*. *Biochem J.*, 1984. **220**(2): p. 521-527.
8. Cooper, S.M. and Grigor, M.R. *Fatty acid specificities of microsomal*

- acyltransferases esterifying positions -1 and -2 of acylglycerols in mammary glands from lactating rats. Biochem. J., 1980. 187: p. 289-295.*
9. Stein, O. and Stein, Y. *Lipid synthesis, intracellular transport, and secretion. II. Electron microscopic radioautographic study of the mouse lactating mammary gland. J. Cell Biol., 1967. 34: p. 251-263.*
 10. Patton, S. and Jensen, R.G. *Lipid metabolism and membrane functions of the mammary gland. Pages 163-277 in Progress in the Chemistry of Fats and Other Lipids. Vol. XIV, Part 4. R.T. Holman, ed. Pergamon Press, Oxford, United Kingdom., 1975.*
 11. Dylewski, D.P., Dapper, C.H., Valivullah, H.M., Deeney, J.T., and Keenan, T.W. *Morphological and biochemical characterization of possible intracellular precursors of milk lipid globules. Eur. J. Cell Biol., 1984. 35: p. 99-111.*
 12. Zaczek, M. and Keenan, T.W. *Morphological evidence for an endoplasmic reticulum origin of milk lipid globules obtained using lipid-selective staining procedures. Protoplasma., 1990. 159: p. 179-182.*
 13. Ghosal, D., Shappell, N.W., and Keenan, T.W. *Endoplasmic reticulum luminal proteins of rat mammary gland. Potential involvement in lipid droplet assembly during lactation. Biochim. Biophys. Acta, 1994. 1200: p. 175-181.*
 14. Martin, S. and Parton, R.G. *Lipid droplets: a unified view of a dynamic organelle. Nat Rev Mol Cell Biol, 2006. 7(5): p. 373-8.*
 15. Nickerson, S., C., and Keenan, T. W. *Distribution and orientation of microtubules in milk secreting epithelial cells of rat mammary gland. Cell Tiss. Res. 1979. 202;*

P. 303-312.

16. Patton, S. *Reversible suppression of lactation by colchicine*. FEBS Lett., 1974. **48**: p. 85-87.
17. Henderson, A.J. and Peaker, M. *The effects of colchicine on milk secretion, mammary metabolism and blood flow in the goat*. Quart. J. Exp. Physiol., 1980. **65**: p. 367-378.
18. Patton, S., Stemberger, B.H. and Knudson, C.M. *The suppression of milk fat globule secretion by colchicine: an effect coupled to inhibition of exocytosis*. Biochim. Biophys. Acta., 1977. **499**: p. 404-410.
19. Daudet, F., Augeron, C., and Ollivier-Bousquet, M. *Early action of colchicine, ammonium chloride and prolactin, on secretion of milk lipids in the lactating mammary gland*. Eur. J. Cell Biol., 1981. **24**: p. 197-202.
20. Du, Y., Weed, S, A., Xiong, W, C., Marshall, T, D., and Parsons, J, T. *Identification of a novel cortactin SH3 domain-binding protein and its localization to growth cones of cultured neurons*. Mol. Cell Biol, 1998. **18**: p. 5838-5851.
21. Loizzi, R., F., de Pont, J, J., and Bonting, S, L. *Inhibition by cyclic AMP of lactose production in lactating guinea pig mammary gland sliced*. Biochim. Biophys. Acta, 1975. **392**(1): p. 20-25.
22. Patton, S. and Keenan, T.W. *The milk fat globule membrane*. Biochim. Biophys. Acta., 1975. **415**: p. 273-309.
23. Fortunato, D., Giuffrida, M, G., and Cavaletto, M. *Structural protome of human colostrat fat globule membrane proteins*. Proteomics, 2003. **3**: p. 897-905.

24. Bucheim, W. *Paracrystalline arrays of milk fat globule membrane associated proteins as revealed by freeze-fracture*. *Naturwissenschaften*, 1982. **69**: p. 505-507.
25. Mather, I.H., Jack, L.J., Madara, P.J., and Johnson, V.G. *The distribution of MUC1, an apical membrane glycoprotein, in mammary epithelial cells at the resolution of the electron microscope: implications for the mechanism of milk secretion*. *Cell Tiss. Res.*, 2001. **304**(1): p. 91-101.
26. Franke, W.W., Heid, H.W., Grund, C., Winter, S., Freudenstein, C., Schmid, E., Jarasch E.D., and Keenan, T.W. *Antibodies to the major insoluble milk fat globule membrane-associated protein: specific location in apical regions of lactating epithelial cells*. *J. Cell Biol.*, 1981. **89**: p. 485-494.
27. Freudenstein, C., Keenan, T.W., Eigel, W.N., Sasaki, M., Stadler, J., and Frankel, W.W. *Preparation and characterization of the inner coat material associated with fat globule membranes from bovine and human milk*. *Exp. Cell Res.*, 1979. **118**: p. 277-294.
28. Keenan, T.W., and Mather, I.H. *Intracellular origin of milk fat globules and the nature of the milk fat globule membrane*. *Adv. Dairy Chem.-Lipids*, 2006. **2**: p. 137-171.
29. Jhanwar, A. *Isolation and characterization of different aggregates of lipid from bovine milk*, M.S. thesis. 2009, Utah State Univ.
30. Walstra, P. *Studies on milk fat dispersion. II. Globule-size distribution of cows milk*. *Netherlands Milk and Dairy Journal*, 1969. **23**: p. 99-110.
31. Attaie, R., Richter, R. L. , *Size distribution of fat globules in goat milk*. *J. Dairy Sci*,

2000. **83**: p. 940-944.
32. Simonin, C., Ruegg, M. and Sidiropoulos, D. *Comparison of the fat content and fat globule size distribution of breast milk from mothers delivering term and preterm.* Amer. J. Clin. Nutr. , 1984. **40**(820-826).
 33. Chung, S., Brown, M, J., Sandberg, B, M., and McIntosh, M. *Trans-10,cis-12 CLA increases adipocyte lipolysis and alters lipid droplet-associated proteins: role of mTOR and ERK signaling.* J. Lipid Res., 2005. **46**: p. 885-895.
 34. Hvarregaard, J., Andersen, H.M., Berglund, L., Rasmussen, J.T., and Petersen, T.E. *Characterization of glycoprotein PAS-6/7 from membranes of bovine milk fat globules.* Eur. J. Biochem., 1996. **240**: p. 628-636.
 35. Mather, I.H. *A review and proposed nomenclature for major proteins of the milk-fat globule membrane.* J. Dairy Sci., 2000. **83**(2): p. 203-47.
 36. Jeong, J., Rao, A.U., Xu, J., Ogg, S.L., Hathout, Y., Fenselau, C., and Mather, I.H. *The PRY/SRY/B30.2 domain of butyrophilin 1a1 (Btn1a1) binds to xanthine oxidoreductase: Implications for the function of Btn1a1 in the mammary gland and other tissues.* J. Biol. Chem., 2009. **284**: p. 22444-22456.
 37. Spitsberg, V.L., Matitashvili, E., and Gorewit, R.C. *Association and coexpression of fatty-acid-binding protein and glycoprotein CD36 in the bovine mammary gland.* Eur. J. Biochem., 1995. **230**: p. 872-878.
 38. Spicer, A.P., Rowse, G.J., Linder, T.K., and Gendler, S.J. *Delayed mammary tumor progression in Muc-1 null mice.* J. Biol. Chem., 1995. **270**: p. 30093-30101.
 39. Mather, I.H. 2011. Milk Lipids: Milk fat globule membrane, *in* Encyclopedia of

- Dairy Sciences, Fuquay, J.W., Fox, P.F., and McSweeney, P.L.H. (Eds.), pp 680-690, (Second Edition).
40. Tazi-Ahnini, R., Henry, J., Offer, C., Bouissou-Bouchouata, C., Mather, I.H., and Pontarotti, P. *Cloning, localization, and structure of new members of the butyrophilin gene family in the juxta-telomeric region of the major histocompatibility complex*. Immunogenetics, 1997. **47**: p. 55-63.
 41. Banghart, L.R., Chamberlain, C.W., Velarde, J., Korobko, I.V., Ogg, S.L., Jack, L.J., Vakharia, V.N. and Mather, I.H. *Butyrophilin is expressed in mammary epithelial cells from a single-sized messenger RNA as a type I membrane glycoprotein*. J. Biol. Chem., 1998. **273**: p. 4171-4179.
 42. Nguyen, T., Liu, X.K., Zhang, Y., and Dong, C. *BTNL2, a butyrophilin-like molecule that functions to inhibit T cell activation*. J Immunol, 2006. **176**(12): p. 7354-60.
 43. Guggenmos, J., Schubart, A.S., Ogg, S., Andersson, M., Olsson, T., Mather, I.H., and Linington, C. *Antibody cross-reactivity between myelin oligodendrocyte glycoprotein and the milk protein butyrophilin in multiple sclerosis*. J. Immunol., 2004. **172**: p. 661-668.
 44. Leo, C.J., Anthony, H.K., Zahra, K., Rhodes, D, A., and Trowsdale, J. *Structural basis for PRYSPRY-mediated tripartite motif (TRIM) protein function*. Proc Natl Acad Sci USA., 2007. **104**: p. 6200-6205.
 45. Ogg, S.L., Weldon, A.K., Dobbie, L., Smith, A.J., and Mather, I.H. *Expression of butyrophilin (Btn1a1) in lactating mammary gland is essential for the regulated*

- secretion of milk-lipid droplets*. Proc. Natl. Acad. Sci. U S A, 2004. **101**(27): p. 10084-10089.
46. Vorbach, C., Capecchi, M, R., and Penninger, J, M. *Evolution of the mammary gland from the innate immune system? .* BioEssays, 2006. **28**: p. 606-616.
47. Wang, W., Lv, N., Zhang, S., Shui, G., Qian, H., Zhang, J., Chen, Y., Ye, J., Xie, Y., Shen, Y., Wenk, M,R., and Li, P. *Cidea is an essential transcriptional coactivator regulating mammary gland secretion of milk lipids*. Nat. Med., 2012. **18**(2): p. 235-243.
48. Vorbach, C., Scriven, A. and Capecchi, M.R. *The housekeeping gene xanthine oxidoreductase is necessary for milk fat droplet enveloping and secretion: gene sharing in the lactating mammary gland*. Genes Develop., 2002. **16**(24): p. 3223-3235.
49. Greenwalt, D.E., Lpsky, R.H., Ockenhouse, C.F., Ikeda, H., Tandon, N.N., and Jamieson, G.A. *Membrane glycoprotein CD36: a review of its roles in adherence, signal transduction, and transfusion medicine*. Blood, 1992. **80**: p. 1105-1115.
50. Chong, B.M., Russel, D. T., Schaack, J., Orlicky, J. D., Reigan. P., Ladinsky, M., and McManaman, L. J., *The adipophilin C-terminus is a self-folding membrane binding domain that is important for milk lipid secretion. .* J. Biol. Chem., 2011. **286**: p. 23254-23265.
51. McManaman, J.L., Palmer, C.A., Wright, R.M., and Neville, M.C. *Functional regulation of xanthine oxidoreductase expression and localization in the mouse mammary gland: evidence of a role in lipid secretion*. J. Physiol., 2002. **545**(2): p.

- 567-579.
52. Russell, D., T., Schaack, J., Orlicky, J, D., Palmer, C., Chang, J, B., Chan, L., and McManman, L, J. *Adipophilin regulates maturation of cytoplasmic lipid droplets and alveolae in differentiating mammary glands*. J. Cell Sci. , 2011. **124**: p. 1-7.
 53. Aoki, Y., and Nakagawa, Y. *Weaning-induced expression of a milk-fat globule protein, MFG-E8, in mouse mammary glands, as demonstrated by the analyses of its mRNA, protein and phosphatidylserine-binding activity*. Biochem. J., 2006. **395**: p. 21-30.
 54. Wooding, F.B.P. *The mechanism of secretion of the milk fat globule*. J. Cell Sci., 1971. **9**: p. 805-821.
 55. Robenek, H., Hofnagel, O., Buers, I., Lorkowski, S., Schnoor, M., Robenek, M.J., Heid, H., Troyer, D., and Severs, N.J. *Butyrophilin controls milk fat globule secretion*. Proc Natl Acad Sci U S A, 2006. **103**(27): p. 10385-10390.
 56. Smith, P., K., Krohn, R,I., Hermanson, G,T., Mallia, A,K., Gartner, F,H., Provenzano, M,D., Fujimoto, E,K., Goeke, N,M., Olson, B,J., and Klenk, D,C. *Measurement of protein using bicinchoninic acid*. Anal. Biochem., 1987. **150**(1): p. 76-85.
 57. Eder, K., Reichlmayr-Lais, M,A., and KirchgeBner, M. *Studies on the extraction of phospholipids from erythrocyte membranes in the rat*. Clin Chim Acta, 1993. **219**(1-2): p. 93-104.
 58. Shapiro, A., L., Viñuela, E., and Maizel, J,V, Jr. *Molecular weight estimation of polypeptide chains by electrophoresis in SDS-polyacrylamide gels*. Biochem

- Biophys Res Commun, 1967. **28**(5): p. 815-820.
59. Towbin, H., Staehelin, T., and Gordon, J. *Electrophoretic transfer of proteins from polyacrylamide gels to nitrocellulose sheets: procedure and some applications.* Proc. Natl. Acad. Sci. U.S.A., 1979. **76**: p. 4350-4354.
60. Ohsaki, Y., Maeda, T., and Fujimoto, T. , *Fixation and permeabilization protocol is critical for the immunolabeling of lipid droplet proteins.* Histochem. Cell. Biol., 2005. **124**: p. 445-452.
61. Huppertz, T., and Kell, A.L. *Physical chemistry of milk fat globules. Advanced Dairy Chemistry.* Lipids, 2006. **2**: p. 173-212.
62. Ma, Y., and Barbano, M, D. *Gravity separation of raw bovine milk: fat globule size.* J Dairy Sci., 2000. **83**: p. 1719-1727.
63. Gouedranche, H., Fauquant, J., and Maubois, J.L. *Fractionation of globular milk fat by membrane microfiltration.* Lait, 2000. **80**: p. 93-98.
64. Patton, S. and G.E. Huston, *A method for isolation of milk fat globules.* Lipids., 1986. **21**: p. 170-174.
65. El-Loly, M. M. *Composition, properties and nutritional aspects of milk fat globule membrane -a review.* Pol.J.Food Nutr.Sci., 2011. **61**(1): p. 7-32.
66. Van Gaal, E., V., Spierenburg, G., Hennink, W,E., Crommelin, D,J., and Mastrobattista, E. *Flow cytometry for rapid size determination and sorting of nucleic acid containing nanoparticles in biological fluids.* J Control Release, 2010. **141**(3): p. 328-338.

67. Jacob, J., *The potential role of butyrophilin and xanthine oxidoreductase in controlling the amount and size of milkfat droplets*. M.S. thesis, 2008. Univ. of Maryland.
68. Lopes, C., and Menard, O., *Human milk fat globules: polar lipid composition and in situ structural investigations revealing the heterogeneous distribution of proteins and the lateral segregation of sphingomyelin in the biological membrane*. *Colloids and Surfaces B: Biointerfaces*, 2011. **83**: p. 29-41.
69. Lopez, C., Madec, M., and Flores, J.R., *Lipid rafts in the bovine milk fat globule membrane revealed by the lateral segregation of phospholipids and heterogeneous distribution of glycoproteins*. *Food Chemistry*, 2010. **120**: p. 22-33.
70. Lopez, C., *Milk fat globules enveloped by their biological membrane: Unique colloidal assemblies with a specific composition and structure*. *Current Opinion in Colloid & Interface Science*, 2011. **16**(5): p. 391-404.
71. Huang, B., Bates, M., and Zhuang, X., *Super-resolution fluorescence microscopy*. *Annu. Rev. Biochem.*, 2009. **78**: p. 993-1016.
72. Febbraio, M., Abumrad, N.A., Haiar, D.P., Sharma, K., Cheng, W., Pearce, S.F., and Silverstein, R.L. *A null mutation in murine CD36 reveals an important role in fatty acid and lipoprotein metabolism*, *J. Biol. Chem.* 1999. **274** (27): 19055-19062.